



The Monte San Nicola section (Sicily) revisited: A potential unit-stratotype of the Gelasian Stage

L. Capraro ^{a,*}, S. Bonomo ^b, A. Di Stefano ^c, P. Ferretti ^d, E. Fornaciari ^a, S. Galeotti ^e, A. Incarbona ^f, P. Macri ^g, I. Raffi ^h, N. Sabatino ⁱ, F. Speranza ^g, M. Sprovieri ⁱ, E. Di Stefano ^f, R. Sprovieri ^f, D. Rio ^a

^a Dipartimento di Geoscienze, Università Degli Studi di Padova, Via G. Gradenigo 6, 35131, Padova, Italy

^b Istituto di Geologia Ambientale e Geoingegneria (CNR-IGAG), Area Della Ricerca di Roma 1- Strada Provinciale 35d, 9-00010, Montelibretti, RM, Italy

^c Dipartimento di Scienze Biologiche, Geologiche e Ambientali, Università Degli Studi di Catania, Corso Italia 57, 95100, Catania, Italy

^d Dipartimento di Scienze Ambientali, Informatica e Statistica, Università Ca' Foscari di Venezia, Via Torino 155, 30172, Venezia, Italy

^e Dipartimento di Scienze Pure e Applicate, Università Degli Studi di Urbino, Via Ca' Le Suore 2-4, 61029, Urbino, Italy

^f Dipartimento di Scienze Della Terra e Del Mare, Via Archirafi 22, 90123, Palermo, Italy

^g Istituto Nazionale di Geofisica e Vulcanologia (INGV), Via di Vigna Murata 605, 00143, Roma, Italy

^h Dipartimento di Ingegneria e Geologia, Università Degli Studi "G. D'Annunzio" di Chieti-Pescara, Via Dei Vestini, 66100, Chieti, Italy

ⁱ IAS-CNR, Via Del Mare 3, 91021, Torretta Granitola, Campobello di Mazara, Trapani, Italy

ARTICLE INFO

Article history:

Received 20 August 2021

Received in revised form

14 December 2021

Accepted 29 December 2021

Available online 17 January 2022

Handling Editor: Professor Xiaoping Yang

ABSTRACT

The Monte San Nicola area (Southern Sicily) offers a spectacular exposure of open-marine sediments that were employed in 1998 for defining the Global Stratotype Section and Point (GSSP) of the Gelasian Stage (Upper Pliocene). After the lowering of the Pliocene/Pleistocene boundary to ca. 2.6 Ma in 2010, the Gelasian GSSP has been redefined as the base of both the Pleistocene Series and the Quaternary Period, which increased its importance and visibility within the scientific community. However, documentation on the Monte San Nicola reference section is still sparse. In the light of its renewed status, we decided to undertake a complete revision of the Gelasian Stage in its type area, in order to evaluate whether the succession of bio- and magnetostratigraphic events that are expected to occur in the interval of relevance are represented adequately in the local record. The results of our investigation demonstrate that the Monte San Nicola succession spans continuously from the upper Piacenzian to the lower Calabrian, and is therefore suitable to host the Unit Stratotype, or even the Astronomical Unit Stratotype, of the Gelasian Stage.

© 2022 Elsevier Ltd. All rights reserved.

1. Introduction

Following a debated resolution ratified by the International Union on Geological Sciences (IUGS) in 2009 (Gibbard and Head, 2010; Gibbard et al., 2010), the base of both the Pleistocene Series/Epoch and the Quaternary System/Period, previously defined as corresponding to the GSSP of the Calabrian Stage (1.806 Ma; Cita et al., 2008; 2012), have been lowered to match the base of the Gelasian Stage (2.588 Ma; Rio et al., 1994; 1998). The decision was essentially founded on questionable climatostratigraphic motivations (Raffi et al., 2020), as the proponents implied that the base of

the Gelasian would provide, in terms of global relevance and correlation potential, a more logical and effective chronostratigraphic reference for establishing the beginning of the Quaternary than the base of the Calabrian (Gibbard and Head, 2010; Gibbard et al., 2010). Indeed, the Gelasian GSSP approximates a cluster of prominent "cold" episodes (i.e., the MIS 100-MIS 96 interval) interpreted as the global climatic response to the definitive onset of large and stable ice sheets in the northern hemisphere (Lisiecki and Raymo, 2005). Consequently, both the Pliocene Series and the Neogene Period were truncated at the top of the Piacenzian Stage, and the Gelasian Stage was reclaimed as the basal chronostratigraphic unit of the Quaternary. Since the beginning of the Quaternary coincides with the base of the Pleistocene (Walsh, 2008), the base of the Gelasian presently marks the beginning of the Pleistocene Epoch as well (Gradstein et al., 2020).

* Corresponding author.

E-mail address: luca.capraro@unipd.it (L. Capraro).

Although there is still no unanimous view on the solution, we welcome the renewed popularity of the Gelasian Stage within the scientific community over the past few years. Yet, there is no denying that the available documentation on the Monte San Nicola section, where the GSSP of the Gelasian Stage was established, is anything but complete and up to date. The only dedicated paper we are aware of, in addition to those of [Rio et al. \(1994, 1998\)](#), is that published by [Becker et al. \(2005\)](#), which was only focused on a ca. 4 m-long interval (MIS 101-MIS 99) out of the >75 m that constitute the local Gelasian succession. With this awareness in mind, we recently decided to undertake a complete revision of the Monte San Nicola stratigraphy. In this paper we present the unpublished results obtained via the investigation of two sections, these being the “historical” Monte San Nicola section, where the GSSP of the Gelasian Stage was established ([Rio et al., 1998](#)), and a novel profile located nearby. Ultimate goal of our research is providing evidence that the Monte San Nicola section offers an undisturbed and well-documented stratigraphic record extending continuously from the top of the Piacenzian up to the base of the Calabrian. This analysis is a basic requirement to establish whether the local succession is suitable to host the Unit Stratotype of the Gelasian Stage, other than its GSSP.

1.1. The Gelasian stage: historical remarks

The idea of establishing a third Stage for the Pliocene Series above the Piacenzian, what would later become the Gelasian Stage, was originally conceived in the Arda Valley (Piacenza Province, Northwestern Italy), probably the most classical area in the world for the Pliocene Series. The richly fossiliferous marine succession exposed along the Arda river was employed by [Brocchi \(1814\)](#) for establishing the “Subappennine Unit”, which was later referred to by [Lyell \(1833\)](#) as the marine “type” for the “Older Pliocene”. The same stratigraphy has also been considered as the reference for defining the Piacenzian Stage ([Mayer-Eymar, 1858](#); [Pareto, 1865](#); [Barbieri, 1967](#)). In the late 1980’s, [Raffi et al. \(1989\)](#) and [Rio et al. \(1988\)](#) re-examined the Pliocene to Pleistocene marine succession of the Val d’Arda-Castell’Arquato area to discover that the transition from the top of the Piacenzian stratotype (as defined by [Barbieri, 1967](#)) and the overlying regressive “yellow sands” (the “Astian” *Auctorum*) is close in age to the global climate cooling documented at about 2.6 Ma. In the wake of these findings, [Rio et al. \(1988, 1991\)](#) argued against the universally followed practice (e.g., [Barbieri, 1967](#); [Cita, 1973](#); [Berggren et al., 1985](#)) of extending the Piacenzian up to the base of the Pleistocene, i.e., up to the first occurrence of the so-called “Northern guests” in the Mediterranean marine sections, at ca. 1.8–1.6 Ma ([Pasini and Colalongo, 1997](#)). Instead, they proposed a threefold subdivision of the Pliocene, with the introduction of a new Stage corresponding to the “Astian” (Late Pliocene) of Castell’Arquato. The “historical” sections of the Arda Valley, however, are mainly composed of shallow-water marine sandstones, inadequate to serve as GSSP sections ([Hedberg, 1976](#); [Salvador, 1994](#)). Hence, [Rio et al. \(1994\)](#) proposed to establish the new Stage, the “Gelasian”, in the Monte San Nicola section (near Gela, southern Sicily), in the same area where the GSSPs of the Zanclean (Eraclea Minoa section; [Van Couvering et al., 2000](#)) and Piacenzian (Punta Piccola section; [Castradori et al., 1998](#)) are also located. The Monte San Nicola stratigraphy is represented by a continuous, fossiliferous and well exposed succession of open-marine muds, which also provided a sound magnetostratigraphic record in the critical interval straddling the Piacenzian-Gelasian boundary ([Channell et al., 1992](#)). The section preserves a complete record of Mediterranean Precession-related Sapropels (MPRS) that allows for an astronomical age calibration of the boundary: it is no coincidence that the Monte San Nicola section was employed for

reconstructing the Astronomical Time Scale (ATS) for the late Neogene ([Hilgen, 1991a, 1991b, 1999](#)).

1.2. The Gelasian stage of monte San Nicola: previous studies and definition

The first “modern” scientific report on the Monte San Nicola succession was that carried out by [Spaak \(1983\)](#). This pioneering study was followed by those of [Sprovieri et al. \(1986\)](#) and [Howell et al. \(1988\)](#), who mainly focused on the laminated intervals preserved in the Monte San Nicola section. [Bertoldi et al. \(1989\)](#) analyzed the pollen content of the lower part of the succession as a segment of a long Central Mediterranean composite record, in the attempt of reconstructing the long-term climatic evolution in the region during the late Neogene. The first integrated and comprehensive study of the Monte San Nicola section was made by [Channell et al. \(1992\)](#), who studied the very same stratigraphic profile of [Spaak \(1983\)](#) and reported on the good magnetic properties and rich micropaleontological content of the local record. In particular, they demonstrated that the Pliocene open marine stratigraphy in the Monte San Nicola area spans from the planktic foraminiferal Zone MPL3 (late Zanclean, >4 Ma) to the upper part of the calcareous nannofossil *Helicosphaera sellii* (MNN19c) Zone (Calabrian, ca. 1.6 Ma). [Rio et al. \(1994\)](#) proposed the profile described by [Channell et al. \(1992\)](#) as the most suitable section for defining the GSSP of the Upper Pliocene Stage, the “Gelasian”. The GSSP was soon ratified ([Rio et al., 1998](#)) and located at the very base of the marly unit that overlies a prominent laminated layer, known as “Nicola bed” (after Monte San Nicola). The latter is correlative to the MPRS 250 (i-cycle 250) of [Lourens et al. \(1996\)](#), that was deposited during the interglacial Marine Isotopic Stage (MIS) 103. The astronomically-calibrated age of the boundary is 2.588 Ma ([Hilgen, 1991b](#); [Rio et al., 1998](#)). According to the definition of [Rio et al. \(1998\)](#), the Piacenzian-Gelasian boundary is located 1 m above the Gauss-Matuyama geomagnetic reversal, and slightly below the highest occurrence of the calcareous nannofossil *Discoaster pentaradiatus* (MIS 99) and the lowest occurrence of the planktonic foraminifer *Globorotalia bononiensis* (MIS 96). The boundary is also approximated by the period of global climate cooling associated to the cluster of prominent glacial events between MIS 100 and MIS 96 ([Lisiecki and Raymo, 2005](#)). [Becker et al. \(2005\)](#) performed a high-resolution investigation across the MIS 100 glacial in a stratigraphic section different from the classical profile of [Channell et al. \(1992\)](#). Their results show that a high-frequency climatic variability exists across the glacial event in the sub-milankovian frequency spectrum of 5–8 kyr/cycle, which is reminiscent of the Heinrich and Dansgaard-Oeschger events of the late Pleistocene ([Dansgaard et al., 1993](#); [Heinrich, 1988](#); [Mayewski et al., 1997](#)). [Herbert et al. \(2015\)](#) analyzed the alkenone record from the Monte San Nicola succession, and concluded that the most significant and consistent drop in SST in the Central Mediterranean took place at ca. 1.84 Ma, very close to the historical Pliocene/Pleistocene (i.e., Gelasian/Calabrian) boundary. However, a prolonged and severe cold spell occurred during MIS 78 (ca. 2.09 Ma), consistent in time with the “first deep glaciation” of [Rohling et al. \(2014\)](#). Interestingly, the MIS 100-MIS 96 interval, which is often referred to as “the beginning of the ice ages” (e.g., [Shackleton et al., 1984](#)), appears in their record as a transient, short-term cooling episode that apparently did not initiate a long-term decrease in SSTs over the Central Mediterranean ([Herbert et al., 2015](#)).

1.3. Geologic setting

The area of Monte San Nicola is located in the southeastern part of the Caltanissetta sedimentary basin, ca. 6 km inland from the

coast (Fig. 1). The Caltanissetta Basin is a late Neogene structure confined by the front of the Maghrebic-Apennine Chain, to the west, and the Hyblean Foreland, to the east (Catalano et al., 2013; Lentini and Carbone, 2014). It consists of a single thrust sheet containing a train of continuously tightening folds (Lickorish et al., 1999) that constitute the central salient part of the “Gela Nappe” (Beneo, 1958; Ogniben, 1969). The latter includes an heterogeneous assortment of sedimentary units, ranging from the Cretaceous-Eocene “Argille Scagliose” (Ogniben, 1969) to the Serravallian-Tortonian “Numidian Flysch” (Auctorum, Gasparo Morticelli et al., 2015; Pinter et al., 2016, 2018). Complex compressive-translational and rotational movements occurring within the Caltanissetta basin promoted the formation and development of several small piggy-back basins, where an expanded upper Neogene stratigraphy was accommodated (Ogniben, 1969; Catalano et al., 1977; Grasso et al., 1987; Lentini et al., 1991; Vitale, 1996; Lickorish et al., 1999; Ghisetti et al., 2009; Gasparo Morticelli et al., 2015).

The Pliocene to Pleistocene succession is characterized by a shallowing-upward trend, as the basal open-marine hemipelagic sediments show an upward increase in terrigenous content and are eventually capped by a package of shallow-water sandstones that testify the regional uplift. As well as in the Capo Rossello reference area, located ca. 70 km WNW of the study sector (Fig. 1), the open-marine Pliocene and Pleistocene sediments at Monte San Nicola belong to the “Trubi” and “Monte Narbone” Formations. The Trubi Fm (Zanclean-Piacenzian p.p.; Cita and Gartner, 1973; Rio et al., 1984; Castradori et al., 1998), attains here a thickness of ca. 40 m. It consists of a well-bedded succession of off-white marly limestones and grey/beige marls, void of macrofossils, that were laid at an estimated depth of 800–1000 m (Bonaduce and Sprovieri, 1984) and testify the abrupt reprise of deep marine sedimentation after the Messinian salinity crisis (De Visser et al., 1989). Transition to the overlying muds of the Monte Narbone Fm. (Piacenzian p.p.-Calabrian p.p.; Rio et al., 1984; Di Stefano et al., 1993; Caruso, 2004), ca. 125 m thick in the area (Rio et al., 1994), is rapid but gradual. The lithological turnover is associated to a sudden intensification of the terrigenous input, as emphasized by the obvious shift in sediment color to deep blue/tobacco tones and decrease in rock competence. This transition is complemented by the reappearance of sapropel layers, which are not present in the Trubi Fm.

1.4. The Monte San Nicola succession

The hill of Monte San Nicola (37°08′51.4″N, 14°12′16.6″E) attains an altitude of ca. 260 m a.s.l. It is characterized by an asymmetric shape, as its northern slopes are gentle and vegetated, while the southern flank offers a spectacular suite of steep badlands (“calanchi”) that expose the Gelasian succession (Fig. 2). The outcrops can only be reached from the north, as the lowlands surrounding the Monte San Nicola badlands are cultivated and secluded by fences and irrigation canals. The most convenient access to the section is from the “Strada Provinciale” (SP) 8 road, connecting the cities of Gela and Butera, which also offers a complete view on the Monte San Nicola badlands (Fig. 2). A rough track departing southward from the main road leads up to a deserted farmhouse (“Case San Nicola”), from where the crest of Monte San Nicola can be reached after a 15-min walk. This vantage point offers a spectacular view on the underlying stratigraphic succession (Fig. 3). From here, one can appreciate the pervasive sedimentary cyclicity in the lower part of the Monte Narbone Fm. and the upward increase in terrigenous content, revealed by the change in color tones and stratification patterns. It can also be observed that major unconformities and tectonic disturbances are absent, as also confirmed by our extensive field surveys in the area.

In the Monte San Nicola area, only the uppermost portion of the Trubi is preserved, possibly due to tectonic obliteration. As elsewhere (e.g., the Capo Rossello and Punta Piccola sections), the Monte Narbone Fm. at Monte San Nicola can be easily subdivided into two major lithological units, which reflect the upward increase in clay content (Figs. 2 and 3). The lower unit (MN1 hereafter; Fig. 4) is characterized by lighter colors, ranging from off-white to hazel, and includes a well-defined array of thin sedimentary couplets that consist in a clear alternation between darker and lighter layers. Albeit impressive from a distance, this sedimentary cyclicity may be flimsy at a closer inspection, especially on fresh surfaces. In the lowermost part of this unit, MPRS clusters O and A (Verhallen, 1987; Zijdeveld et al., 1991) are clearly visible. The sapropel record of clusters O and A reconstructed at Monte San Nicola was demonstrated to correlate directly with those documented in the Punta Piccola section and other Mediterranean sections (e.g., Hilgen, 1991a, b). The “Nicola bed” (i-cycle 250, MIS 103), the lithological marker of the Gelasian GSSP, is the uppermost sapropel of cluster A (Fig. 3b). Just above, a grey banded interval marks the MIS 100–MIS 96 stratigraphy studied by Becker et al. (2005), that in turn underlies the sapropel layers of cluster B (Verhallen, 1987;

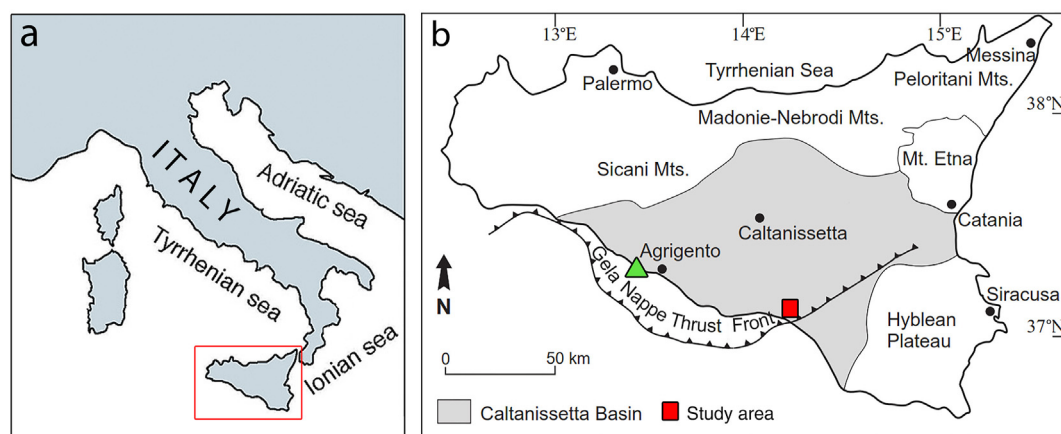


Fig. 1. Location of the study area. a: Sicily is indicated by the red square. b: location of the Monte San Nicola area (in red) in the south-eastern part of the Caltanissetta basin, Sicily (modified from Di Grande and Giandinoto, 2002). The green triangle indicates the position of the area where the reference Capo Rossello composite section was reconstructed (Langereis and Hilgen, 1991). (For interpretation of the references to color in this figure legend, the reader is referred to the Web version of this article.)

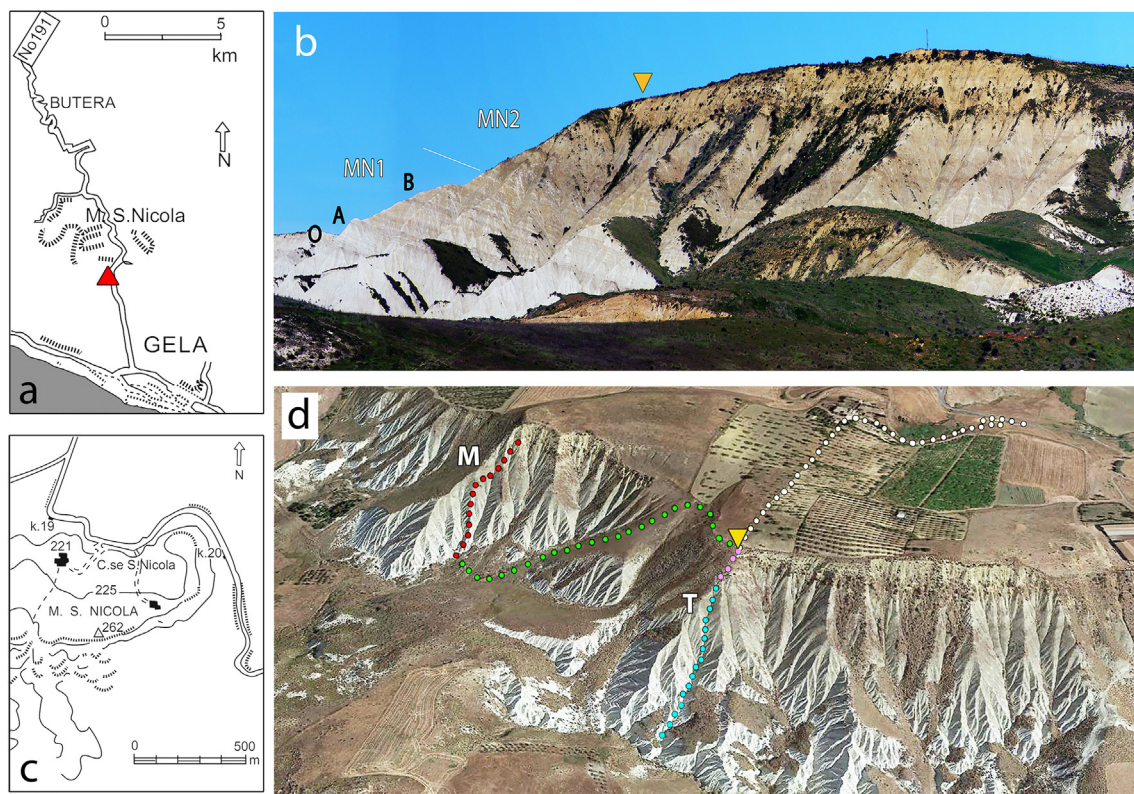


Fig. 2. a) location of the Monte San Nicola area, between the cities of Gela and Butera. The red triangle indicates the stop from where a spectacular view on the Monte San Nicola badlands, shown in panel b, can be observed. From here, sapropel clusters O, A, B and C are clearly visible, as well as the transition from the banded light grey clayey marls of the MN1 unit to the tobacco marly clays of Unit MN2. The “Type” section of Channell et al. (1992) extends below the orange triangle, indicated as “vantage point” in the text. c) sketchmap of the Monte San Nicola area, with indication of the access to the vantage point from the main road. d) 3-D panorama (© Google) on the San Nicola badlands. White dots: access from the main road to the vantage point, indicated by the orange triangle. Pink dots: access to the top of the “Type” section (T, in light blue dots). Green dots: access to the base of the “Mandorlo” section (M, in red dots). (For interpretation of the references to color in this figure legend, the reader is referred to the Web version of this article.)

Zijderveld et al., 1991).

The upper unit (MN2 hereafter; Figs. 2–4) shows a more homogeneous appearance, with duller and darker color tones. From a distance, faint reddish-brownish intercalations are visible (Fig. 3a), that again correspond to laminated sapropel layers. In some instances, they are much thicker here than those observed in the underlying MN1. The succession is finally capped by a ca. 10 to 15 m-thick package of richly fossiliferous marine calcarenites belonging to the Agrigento Fm. *Auctorum* (Calabrian), which testifies the final marine regression before the regional uplift (Motta, 1957; Ruggieri and Greco, 1966; Lickorish et al., 1999).

2. Materials and methods

For this work, we have described and sampled two stratigraphic sections that encompass the entire Gelasian stratigraphy. Both profiles can only be reached descending by foot from the top of the Monte San Nicola hill (Figs. 2 and 4).

The first (“Type” section hereafter) is the classic profile of Channell et al. (1992; base 37°08′45.6″N 14°12′20.6″E, top 37°08′49.6″N 14°12′16.3″E), where the Gelasian GSSP was defined (Rio et al., 1994, 1998). It extends along a steep ravine immediately below the culmination of Monte San Nicola, and cannot be seen in its completeness from above. Advantages of this section are its proximity to the ridge of Monte San Nicola and its historical significance. On the other hand, the profile is very inconvenient as the exposure is locally poor due to vegetation and landslips, especially in the middle part of the succession. Therefore, heavy work and

frequent relocations are needed to attain a continuous stratigraphic record. Furthermore, we detected several joints and cuts in the middle-lower part of the profile that either seem to dislocate, elide or duplicate parts of the stratigraphy. Samples from this section were not subjected to bio- and magnetostratigraphic investigations, because i) the published data provide an adequate background, and ii) tectonics and (locally) poor exposure conditions suggest that the Upper Piacenzian to Lower Calabrian record is not continuous and undisturbed, which is a prerequisite for the scope of this work. Still, we emphasize that the stratigraphic interval where the Gelasian GSSP has been defined is perfectly exposed and completely void of tectonic disturbances.

The second section (“Mandorlo” section hereafter: base 37°08′51.4″N 14°12′00.9″E, top 37°08′55.5″N 14°12′03.1″E) is a new profile located in the western sector of the Monte San Nicola badlands (Figs. 2 and 3), not far from where the short segment investigated by Becker et al. (2005) is located. Main advantages of this section are i) the uninterrupted and very clean exposure, that permits reconstructing a continuous and dependable stratigraphic record throughout the interval of relevance, and ii) the easy and convenient access to the outcrop.

2.1. Sampling

We pinpointed the prominent “Nicola bed” (MPRS A5, i-cycle 250: Verhallen, 1987; Zijderveld et al., 1991; Hilgen, 1991b) as the lithological reference level for our investigation in both sections. In order to ensure an adequate documentation across the Piacenzian-



Fig. 3. a) westward view from the top of Monte San Nicola on the badlands where the “Mandorlo” section was traced (red dots). O, A, B and C indicate sapropel clusters. MN1 and MN2 indicate the two lithozones that constitute the local stratigraphy (see text). b) the basal part of the “Mandorlo” section, with indication of the Nicola bed (NB) at the top of sapropel cluster A. Above, the distinct bedding of the MN1 unit is also visible. (For interpretation of the references to color in this figure legend, the reader is referred to the Web version of this article.)

Gelasian boundary, in the “Mandorlo” section we extended our investigation down to the base of sapropel A2, i.e. 6.25 m below the top of the Nicola bed/Gelasian GSSP (Fig. 4).

Our work routine consisted in removing the weathered rock coating by means of a large hoe, 1 m at a time, in order to expose a fresh and pristine rock surface. After a detailed observation and physical stratigraphic description of the exposure, we collected sediment samples for micropaleontological and geochemical analyses (ca. 700 g each, on average). In both sections, we followed a steady sampling resolution of 33 cm (i.e., 3 samples/m), except for the intervals where exposure conditions were inadequate and/or in the sporadic events of peculiar lithological changes. In total, we collected 260 samples from the “Mandorlo” section (MG-0 to MG-9300) and 209 from the “Type” section (G12-0 to G12-208).

2.2. Calcareous nannofossils

We performed a semi-quantitative study on calcareous nannofossil assemblages to assess the presence/absence of index species in 125 samples from the “Mandorlo” section. Samples were prepared from unprocessed material as smear slides, and examined using a light microscope at 1250x magnification. A preliminary low-resolution survey with an average spacing of 1 m (i.e., one sample out of three) was followed by a more detailed investigation with a 33 cm resolution across the intervals where marker biohorizons were recognized. Analyses were carried out following the methods developed by Thierstein et al. (1977), Rio et al. (1990) and Gardin and Monechi (1998). Specifically, the relative abundances of selected *Gephyrocapsa* species were calculated with respect to a population of at least 300–500 calcareous nannofossil specimens,

while the occurrence of rare but biostratigraphically significant *Discoaster* species was determined by investigating a slide area of ~6 mm². Taxonomic concepts follow those of Perch-Nielsen (1985) and Nannotax (Young et al., 2017) with the exception of the genus *Gephyrocapsa*, for which we followed Rio (1982) and Raffi et al. (1993). Biohorizons have been identified following the regional biostratigraphic scheme of Rio et al. (1990), developed for the Mediterranean Pliocene/Pleistocene record, and the low-middle latitude zonation of Backman et al. (2012). Age estimates for the main biohorizons recognized in the studied record are those proposed by Raffi et al. (2006) and Backman et al. (2012).

2.3. Planktonic foraminifers

We performed a quantitative study on the planktonic foraminiferal assemblages in 257 samples from the “Mandorlo” section. Samples were washed with deionized water using a 63 μm mesh sieve, then oven-dried at 40 °C. Analyses were carried out on split aliquots containing over 400 specimens (on average) from the >125 μm size fraction. Specimens of 18 different species were identified, counted and normalized to percentage values, following the taxonomic concepts of Bolli and Saunders (1985), Hemleben et al. (1989) and Schiebel and Hemleben (2017). A full and updated list of references for taxonomic concepts of taxa relevant for biostratigraphic purposes can be found in Lirer et al. (2019). *Globigerinoides ruber* includes *Globigerinoides elongatus*. *Globigerina bulloides* also includes *Globigerina falconensis*. Bioevents have been identified following the regional biostratigraphic scheme developed for the Mediterranean Pliocene/Pleistocene record, as originally proposed, amended and updated (Cita, 1975; Sprovieri, 1992; Lirer et al., 2019).

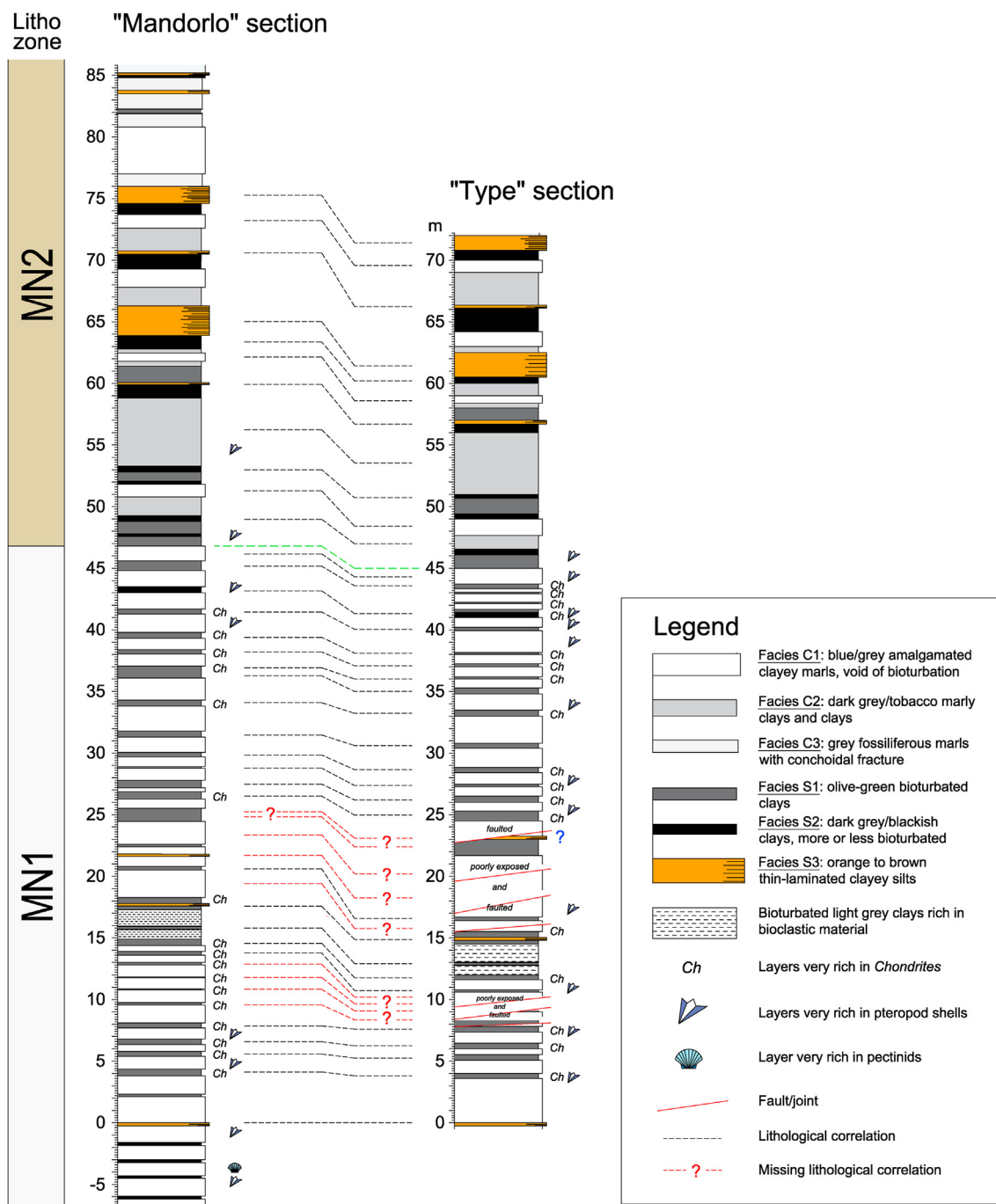


Fig. 4. Simplified stratigraphic logs of the investigated sections. The green dashed line marks the boundary between the MN1 and MN2 units. (For interpretation of the references to color in this figure legend, the reader is referred to the Web version of this article.)

2.4. Magnetostratigraphy

Samples for paleomagnetic analyses were obtained from the "Mandorlo" section by means of a petrol-powered hand corer equipped with a water-cooled core barrel. At first, the selected sampling area was dug deeply in order to remove as much as possible of the weathered coating. Standard-sized mini-cores were drilled into the fresh rock, and oriented in-situ by means of a magnetic compass before extraction. Orientation was corrected to account for the mean magnetic declination of the geomagnetic field in the study area in the year 2006 (i.e., $\sim 2^\circ$ according to Istituto

Nazionale di Geofisica e Vulcanologia -Istituto Nazionale di Geofisica e Vulcanologia, 2001). We collected 88 samples with an average spacing of ca. 60–100 cm. Sampling resolution was higher in the interval straddling the "Nicola bed", where the Gauss/Matuyama geomagnetic reversal was expected to be found (Channell et al., 1992). Samples were transferred to the INGV laboratories in Rome, where the Natural Remanent Magnetization (NRM) was measured using a narrow-access pass-through cryogenic magnetometer 2G Enterprises equipped with three DC SQUID sensors housed in a Lodestar Magnetics shielded room. After NRM measurements, samples were thermally demagnetized in 12 steps

from 20° to 580 °C and the Characteristic remanent magnetization (ChRM) directions were determined using the principal component analysis of Zijderveld (1967).

3. Results and discussion

3.1. Physical stratigraphy

The physical stratigraphic investigation shows that the studied sections preserve a closely comparable stratigraphic record (Fig. 4). Two dominant lithofacies (facies C and S) have been identified, that tend to alternate with repetitive patterns; associated are less common or unique lithotypes that, however, are key for validating the fine-scale correlation between the segments.

3.1.1. Unit MN1

The lower MN1 unit, extending up to ca. 46.8 m in the “Mandorlo” section and 45 m in the “Type” section, is dominated by the hemipelagic clayey marls of sub-facies C1, which are massive and generally devoid of visible bioturbation (Fig. 4). Sediment colors range from light brown/hazel, on weathered surfaces, to deep blue or grey on fresh cuts. Scattered layers of softer grey to tobacco marly clays and harder, grey clayey marls with conchoidal fracture, when dry, are also present. In particular, a conspicuous layer characterized by increased clay content was recognized immediately below sapropel B1 in both the “Mandorlo” and “Type” sections (Fig. 4). Benthic macrofossils such as echinoids, gastropods and bivalves occur sparsely, with the exception of few discrete intervals of concentration. Pteropods are present as rare to abundant throughout, and remarkable concentration levels have been noted and reported in our stratigraphic log (Fig. 4). Benthic meiofaunas (Channell et al., 1992; our data) are rich and diversified. Altogether, facies C1 is indicative of a slope depositional setting subjected to optimal supply of both oxygen and organic matter to the seafloor.

Facies S include three sub-facies (S1 to S3) that occur as discrete layers intercalated within the clayey marls of facies C (Fig. 4). Facies S1 is represented by visibly bioturbated olive-green to dark grey massive clays, soft and sticky, usually very rich in *Chondrites*. This sub-facies is by far the most frequent throughout the MN1 unit.

Facies S2 refers to the prominent intervals of brown, coarsely bioturbated silty clays, correlative to MPRS layers A2 to A4/5 of cluster A, that are located in the basal portion of the MN1 unit (between -6.25 and -1.80 m). Bioturbation is very visible, as burrows are frequently filled with light sediments, dragged from the overlying muds of facies A, that stand out against the darker matrix.

Facies S3 indicates the thin-laminated sapropel layer A5 (namely, the “Nicola bed”) and those of cluster B (between 17.6 and 21.8 m; Fig. 4). Locally, these laminites contain plenty of *Orbulina universa* tests visible to the naked eye.

As a whole, by comparison to analogs found in the central Mediterranean area (e.g., Pasini and Colalongo, 1997; Capraro et al., 2011), facies S points to conditions of reduced oxygen availability and increased organic matter preservation at the seafloor. This scenario is arguably associated to periods of increased stratification of the water column in response to insolation maxima that, eventually, might lead to oxygen starvation in the deeper sectors of the basin (e.g., Rohling et al., 2015). Specifically, facies S1 and S2 are indicative of more or less pronounced disoxia at the seafloor, with the development of opportunistic benthic communities thriving in oxygen-poor environments (Bromley and Ekdale, 1984). Instead, the pristine preservation of fine-scale sedimentary structures (laminae) in facies S3 implies the total suppression of benthic communities, a scenario consistent with periods of anoxia in the deeper parts of the basin (e.g., Raffi and Thunell, 1996; Rohling

et al., 2015). Accordingly, we informally defined the intervals of facies S3 as “true” sapropels (=full anoxic conditions), the brown layers of facies S2 as “failed” sapropels (=severe disoxia), and the greenish clays of facies S1 (either with or without *Chondrites*) as “missing” sapropels (=moderate disoxia).

3.1.2. Unit MN2

A shift in sediment colors toward darker and brownish tones, as well as the waning of small-scale sedimentary cycles, mark the base of the MN2 unit (Fig. 4). This change in sedimentation style and patterns can be interpreted as the transition to an upper slope/outer shelf depositional setting subjected to increased sediment yield with respect to the underlying MN1.

The pervasive cyclicity that occurs throughout unit MN1 is here flimsy. This interval is dominated by facies C2, represented by dark-grey to dark-tobacco marly clays and clays that turn to lighter hues in the upper part of the investigated stratigraphy. Packages of facies C1 occur sporadically. In this segment, all sapropel layers are thin-laminated and reddish/brown in color (facies S3). They are usually underlain by a package of blackish clays of facies S2, which we interpret as the early steps towards the development of full anoxic conditions within the basin. However, facies S2 is also found as discrete layers in the lower part of the MN2 unit. Sapropel layers occur in two bundles of 4 and 2, respectively. Two of them are exceptionally thick, in the order of 1.5–2 m (Fig. 4). Their facies, distribution pattern and stratigraphic position are fully comparable to those found in the Gelasian and Calabrian open-marine successions of the Crotona Basin (Calabria; e.g., Roda, 1964) and are especially well-exposed in the notorious Vrica section (Pasini et al., 1975; Selli et al., 1977; Pasini and Colalongo, 1997). At the top of the studied section (from ca. 76 m upwards in the “Mandorlo” section), the thickness of individual sapropels decreases as the overall sediment color turns lighter again. The dark grey/tobacco marly clays of Facies C2 are replaced by fossiliferous grey silty marls with conchoidal fracture, which we refer to as Facies C3 (Fig. 4).

Our data suggest that, in the interval of relevance, the “Mandorlo” section is ca. 5 m thicker than the “Type” section (i.e., 79 m vs. 74 m). Correlation between the stratigraphic records indicates that this disagreement is primarily due to the pervasive faulting recognized in the “Type” section between ca. 8 and 25 m (Fig. 4). In spite of our scrupulous physical stratigraphic investigation, we could not locate the thin sapropel layer reported as B* by Becker et al. (2005), which is expected to occur between sapropels B1 and B2. An uneven topography of the basin floor, small-scale variations in the intensity and direction of currents and/or erratic terrigenous inputs may provide an explanation for these dissimilarities, which however do not undermine the excellent correlation potential across the Monte San Nicola badlands.

3.2. Calcareous nannofossils

The “Mandorlo” section contains common to abundant calcareous nannofossils with rich, diversified and generally well-preserved assemblages. They are largely dominated by placoliths belonging to genera *Reticulofenestra* and *Dictyococcites*, while *Coccolithus* and *Calcidiscus* are common. *Helicosphaera* specimens are also an important component of the assemblages. On the contrary, specimens belonging to *Discoaster*, *Braarudosphaera*, *Pontosphaera*, *Rabdosphaera*, *Syracosphaera*, *Umbilicosphaera* and *Thoracosphaera* represent secondary components, often very rare. Reworking is common throughout the section, as emphasized by the common presence of Paleogene and Miocene *Discoaster* specimens. In Fig. 5 we report the semi-quantitative distribution patterns of indigenous index species. Three calcareous nannofossil biohorizons of the adopted Zonations (Top *Discoaster pentaradiatus*,

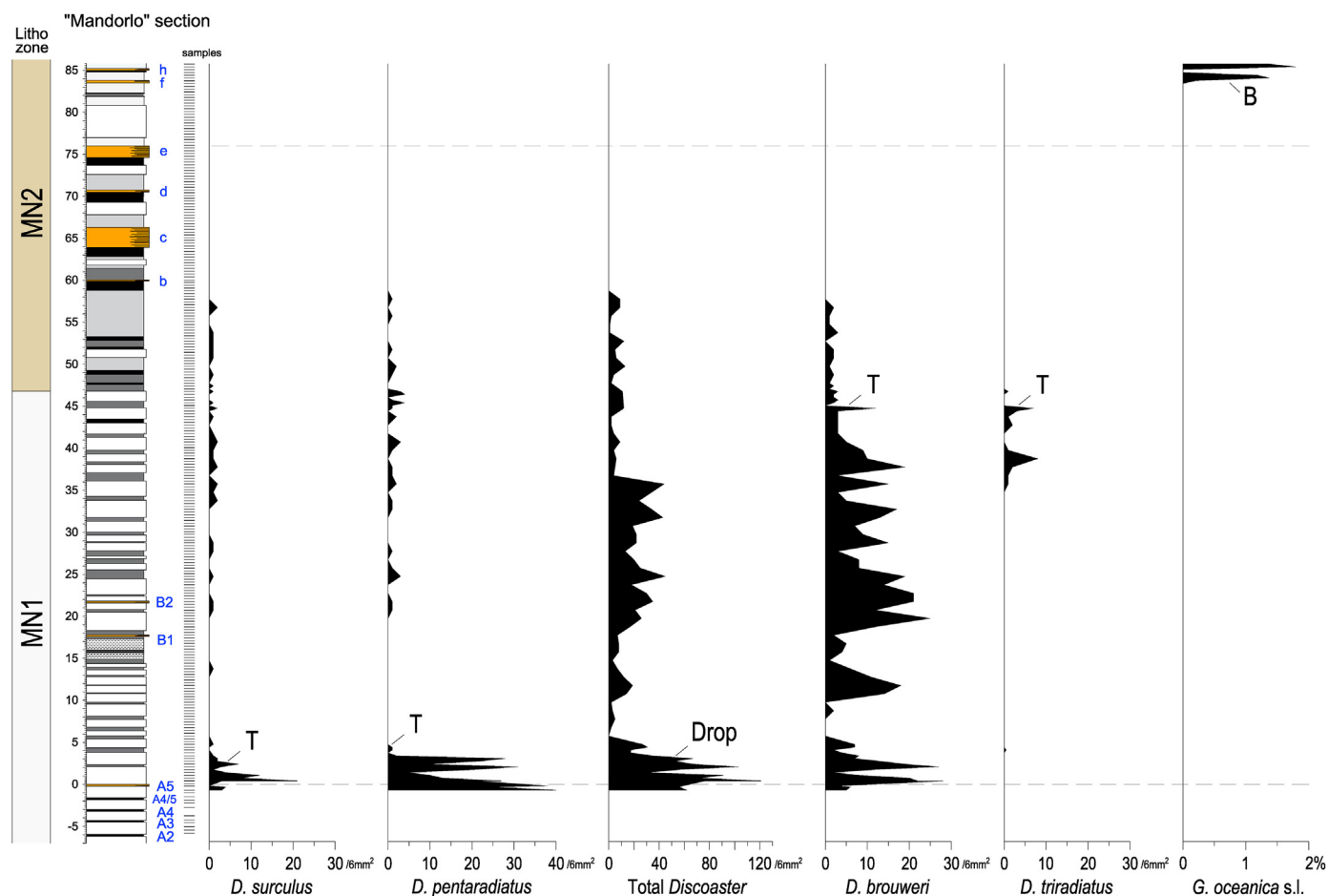


Fig. 5. Semi-quantitative distribution of selected nanofossil taxa with biostratigraphic significance found in the “Mandorlo” section. Values are given in number of individuals counted in a slide area of $\sim 6 \text{ mm}^2$ with the exception of *G. oceanica* s.l., which is reported as percent with respect to a population of ca. 500 calcareous nanofossil specimens. T: Top. B: Base. Blue labels indicate sapropel coding after Verhallen (1987), for clusters A and B, and Selli et al. (1977), for those above (b to h) See text for details. (For interpretation of the references to color in this figure legend, the reader is referred to the Web version of this article.)

Top *Discoaster brouweri* and Base *Gephyrocapsa oceanica* s.l.) and two additional events (Top *Discoaster surculus* and Top *Discoaster triradiatus*) were identified in the “Mandorlo” section. The biohorizon Top *D. pentaradiatus* was pinned at $4.6 \pm 0.16 \text{ m}$ above the Nicola bed, the level that we consider the final exit of the species. This event occurs shortly above the Top *D. surculus* and the top of Gauss Chron (Fig. 5), in good agreement with the literature (e.g., Hilgen, 1991a; Channell et al., 1992; Rio et al., 1997a). Specimens of *D. pentaradiatus* found above its final exit have been considered as reworked. The estimated ages for this biohorizon range from 2.39 Ma in the western tropical Atlantic Ocean to 2.51 Ma in the eastern Mediterranean (MIS 100; Backman et al., 2012; Raffi et al., 2006), which we assume as the fittest chronological reference for our section. The abrupt decline of discoasterids (drop of genus *Discoaster*), delineated by the closely spaced extinctions of *D. surculus* and *D. pentaradiatus*, has been often reported in literature as a useful chronostratigraphic proxy for the Mediterranean (e.g. Driever, 1984, 1988; Rio et al., 1984, 1990; Channell et al., 1992; Di Stefano, 1998). Ages of this event range from 2.50 to 2.54 Ma (Rio et al., 1990; Sprovieri et al., 1998), and has been correlated with the onset of the Northern Hemisphere Glaciation (Backman and Pestiaux, 1987).

At $44.9 \pm 0.16 \text{ m}$ we identified the simultaneous disappearance of *D. brouweri* and *D. triradiatus*, a biohorizon well documented in the literature (e.g. Backman and Shackleton, 1983; Backman et al.,

2012), but usually poorly documented in the Mediterranean, where discoasterids become rare and discontinuous after the extinction of *D. pentaradiatus*. Although in the “Mandorlo” section the recognition of this biohorizon is blurred by reworking, we placed it at about 45 m in the section, where the abundance of *D. brouweri* drops (< 12 specimens in $5\text{--}6 \text{ mm}^2$) and *D. triradiatus* virtually disappears. In the Mediterranean record, the stratigraphic position of these biohorizons with respect to the base of the Olduvai Subchron (ca. 1.945 Ma) is not precisely established, because the available paleomagnetic records are ambiguous (e.g., Tauxe et al., 1983; Zijderveld et al., 1991; Roberts et al., 2010). At ODP Site 652 (Western Mediterranean), *D. brouweri* disappears within the Olduvai (Channell et al., 1990; Glaçon et al., 1990a). In the Vrica section, this species disappears just below the onset of Chron C2n Olduvai (Lourens et al., 1996), while at Singa the Top *D. brouweri* occurs at the base of Olduvai (Hilgen, 1991a). In the classical study on the Monte San Nicola section of Channell et al. (1992), Top *D. brouweri* and Top *D. triradiatus* occur at the base of a normal polarity segment interpreted as corresponding to the Olduvai, which is however preceded by a long interval of undefined polarity. Remarkably, the stratigraphic position of these biohorizons in the “Mandorlo” section is comparable. The age estimate for the Top *D. brouweri*/*D. triradiatus* ranges from 2.06 to 1.93 Ma, 1.95 Ma in the eastern Mediterranean (Raffi et al., 2006; Backman et al., 2012). The Base *G. oceanica* s.l. occurs at $83.91 \pm 0.16 \text{ m}$, within the

uppermost laminated layers documented in the “Mandorlo” section. In the Vrica section, the Base *G. oceanica* s.l. was originally detected above sapropel h (i-cycle 168, 1.71 Ma; Lourens et al., 1996). In the same section, Rio et al. (1997b) recognized this event between the thin sapropel layers f (i-cycle 170) and h (i-cycle 168). Their estimated age is 1.72 Ma, in good agreement with that reported by De Kaenel et al. (1999) for the western Mediterranean. We consider the position of Base *G. oceanica* s.l. as detected in the “Mandorlo” section, in keeping with the occurrence in the reference section of Vrica, calibrated at 1.73 Ma (Raffi et al., 2006).

3.3. Planktonic foraminifera

Planktonic foraminifera assemblages are dominated by *Globigerinoides ruber* (with abundances ranging from 0.3 to 86.2%, 25.7% on average), *Neogloboquadrina incompta* (0.2–78.0%, 13.4% on average), *Globigerina bulloides* (4.9–75.4%, 33.7% on average) and *Globorotalia inflata* (0.0–65.3%, 8.6% on average). Though not dominant, *Orbulina universa* (0.0–32.4%, 6.2% on average) and *Turborotalita quinqueloba* (0.0–28.1%, 4.1% on average) are important components of the assemblages. *Globigerinoides ruber* is a dominant species during interglacial stages (Rio et al., 1998), while the other species prevail during glacial or interglacial cold spells, possibly suggesting the repeated switch in productivity dynamics.

In the “Mandorlo” section (Fig. 6), we unambiguously recognized the complete sequence of planktonic foraminifera events described in the Mediterranean biostratigraphic scheme of Lirer et al. (2019) and observed in reference sections from southern Italy and open Mediterranean Sea in this time interval (e.g., Glaçon

et al., 1990b; Sprovieri et al., 1998; Sprovieri, 1992; Di Stefano et al., 1993).

Three events define major marker biohorizons or zone/subzone boundaries. Namely, these are Base *G. inflata*, Base *Globorotalia truncatulinoides truncatulinoides*, Base common *Neogloboquadrina pachyderma*. The biohorizon Base *G. inflata*, which occurs at ca. 30 m (Fig. 6), defines the base of the MPI6 zone and is associated with MIS 78 and astronomically calibrated at 2.09 Ma (Lourens et al., 1996; Lirer et al., 2019). Base *Globorotalia truncatulinoides truncatulinoides* has been rarely found in the Mediterranean Sea (Cita, 1973; Rio et al., 1984) and is calibrated at 2.00 Ma in open ocean sections. In our record, this bioevent is well documented and occurs very sharply at 37.6 m, at the expected position within the sequence of planktonic foraminifera events (i.e., between the Base and Base common *G. inflata*; Fig. 6). Base common *N. pachyderma*, located at 78.6 m, occurs just above sapropel layer e (Fig. 6), in excellent agreement with the data from the Vrica section (Pasini and Colalongo, 1997; Raffi and Thunell, 1996). The astronomically-calibrated age for this biohorizon is 1.79 Ma (Lourens et al., 2004). The Base common *N. pachyderma*, which approximates the Gelasian/Calabrian boundary and slightly predates the appearance of “northern guests” in the central Mediterranean, follows a long interval of rare and scattered occurrence of the species in the upper Gelasian interval, in agreement with previously recorded distribution ranges (e.g., Sprovieri, 1993; Sprovieri et al., 1998).

Even the ‘auxiliary’ planktonic foraminifera bioevents follow each other in the expected succession (Lirer et al., 2019). Specifically, Top common *Neogloboquadrina atlantica atlantica* is recorded just (ca. 2 m) below Top common *Globorotalia bononiensis* (Fig. 6), a

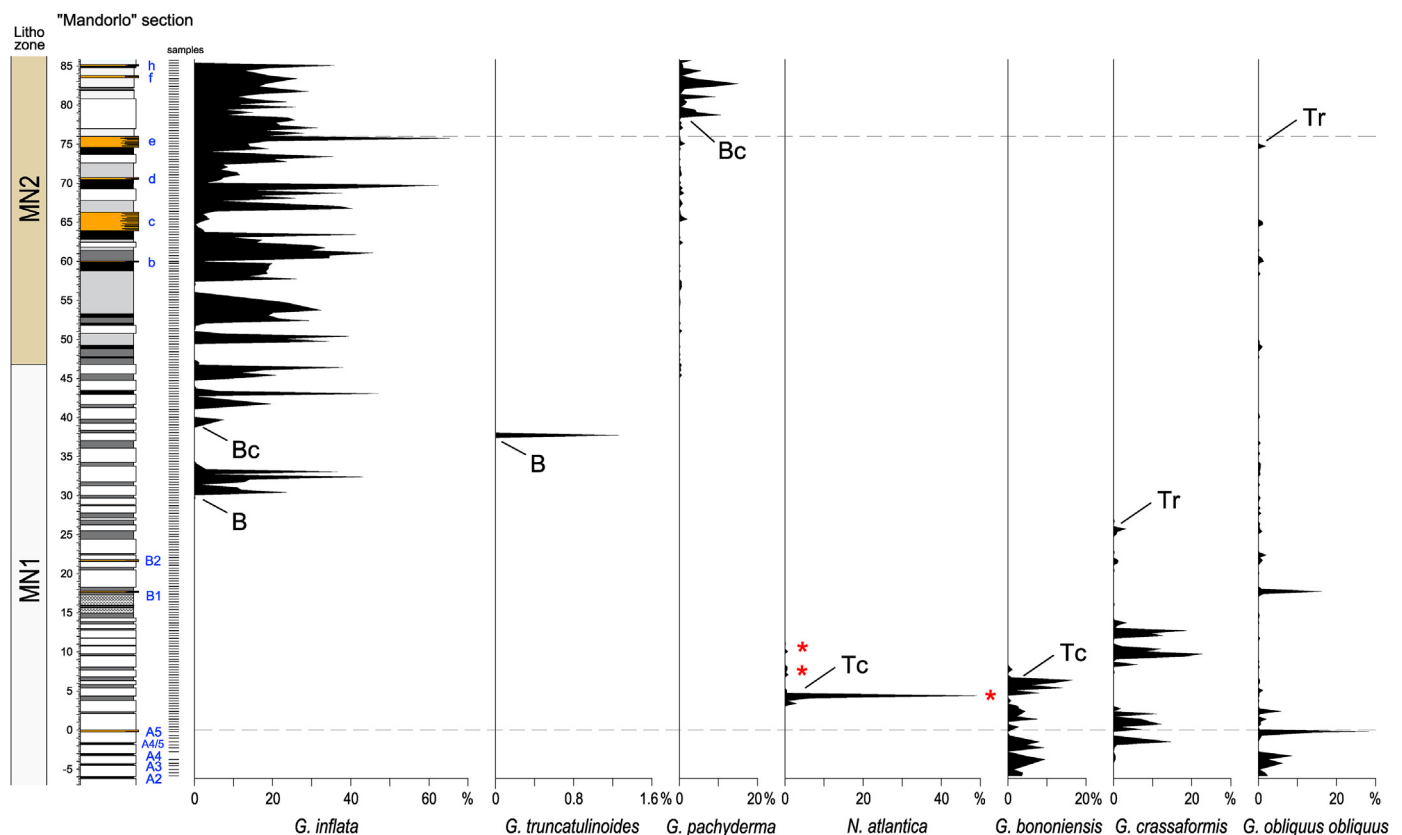


Fig. 6. Relative abundances of selected planktonic foraminiferal species with biostratigraphic significance found in the “Mandorlo” section. Values are given as percent with respect to a population of >300 individuals. The horizontal scale is the same for all species, except for the rare species *G. truncatulinoides*. B: Base. Bc: Base common. T: Top. Tc: Top common. Tr: Top rare. Red asterisks indicate the three influges of *N. atlantica atlantica*. See text for details. (For interpretation of the references to color in this figure legend, the reader is referred to the Web version of this article.)

stratigraphic distance consistent with the expected time gap (1–2 precession cycles) between the two biohorizons (Lirer et al., 2019). The *N. atlantica atlantica* abundance peak of over 40% is associated with MIS 100, while the two smaller peaks immediately above are associated to MIS 98 and 96, as extensively reported in literature (Zachariasse et al., 1990; Lourens et al., 1992; Sprovieri, 1993; Becker et al., 2005; Sprovieri et al., 2006). Noteworthy are Top rare *Globorotalia crassaformis* (at ca. 27 m), and Top rare *Globigerinoides obliquus obliquus* (at 75 m), occurring just below Base common *N. pachyderma* (Fig. 6). However, the stratigraphic position of Top rare *G. obliquus obliquus* in the “Mandorlo” section is ambiguous, and the event was not further considered as a suitable chronological constraint.

3.4. Magnetostratigraphy

Stepwise thermal demagnetization enabled isolation of the ChRM component for 51 samples, often in the 180°–460 °C temperature intervals and with maximum angular deviation (MAD) values less than 10°. Samples characterized by noisy demagnetization behavior in orthogonal vector diagrams (Zijderveld, 1967), and then not sufficiently stable to define a magnetic polarity zonation, have been discarded. The mean ChRM directions for the site section were computed for both normal and reverse polarity values using a maximum likelihood method ($D = 23.2^\circ$, $I = 62.9^\circ$, $k = 8.01$, $\alpha_{95} = 9.0^\circ$).

The ChRM inclination of samples (means about +47° and –53°) mostly oscillates around the expected value for a geocentric axial dipole field at the sampling site latitude. The computed paleomagnetic directions enable to define normal or reverse polarity zonation along the stratigraphic section, with boundaries placed at the mid-point (zero of the ChRM inclination values) of successive opposite polarity samples (Fig. 7). For samples placed between –8.90 (base of the sampled interval) and –0.5 m, the paleomagnetic record has normal polarity (magnetozone N1). Samples between 1.1 and 30.4 m have reverse polarity (magnetozone R1). Within magnetozone R1, samples from 20.2 to 22.5 m indicate a short interval of normal polarity (R1.n1). A long interval of normal polarity (N2) extends from 35.2 to 80.9 m (magnetozone N2). This long interval is characterized by the occurrence of three short-lived intervals (1–2 samples) of reverse polarity (N2.r1, N2.r2, N2.r3). The top of the studied interval, from 81.6 m to 85.6 m, is marked by the return to reverse polarity (reverse magnetozone R2; Fig. 7).

We used the Geomagnetic Polarity Time Scale (GPTS) scheme of Gradstein et al. (2020) to attempt reconstructing an original age model based on our magnetostratigraphic and biostratigraphic records. Polarity ages are after Cande and Kent (1995). The lower magnetozone N1 can be confidently correlated to the Gauss normal Chron C2An (top at 2.581 Ma), while the overlying reverse zone R1 can be correlated to the Matuyama reverse Chron C2r (0.781–2.581 Ma). The midpoint of the Gauss/Matuyama transition is located at ca. 0.3 m above the top of the “Nicola bed” (Fig. 7). These new data confirm and refine the stratigraphic position of the Gauss/Matuyama geomagnetic reversal formerly proposed by Channell et al. (1992) (i.e., about 1 m below the GSSP of the Gelasian Stage).

The normal polarity interval N2 refers to Olduvai normal Chron C2n (1.778–1.945 Ma). Its base is however poorly defined, because many samples in that part of the stratigraphy yielded undefined polarity, being probably affected by overprints. The three short-lived intervals of reverse polarity recognized within the putative Olduvai (N2r1 to N2r3; Fig. 7) are difficult to interpret. It is reasonable to consider that a patchy remagnetization process may have occurred in the host sediment during the early or late

diagenetic stages (e.g. Florindo and Sagnotti, 1996; Sagnotti et al., 2005; Roberts et al., 2011). Further rock magnetic analyses are planned on the section to investigate the possible inconsistency of these few characteristic remanent magnetization directions. However, even though there are no published records of geomagnetic excursions within the Olduvai that can serve as reference for such events, we cannot exclude that they could represent “true” geomagnetic signatures (e.g. the pre-Olduvai, and other cryptochrons also reported in Laj and Channell, 2007). In general, documentation on the Olduvai Subchron in the central Mediterranean region is sparse and inconsistent. In the key Vrica section, paleomagnetic investigations carried out over the years by several Authors across this interval have been demonstrated to provide conflicting results (see discussion in Roberts et al., 2010). Correlation between our paleomagnetic and biostratigraphic records confirms that, other than poorly defined, the base of the Olduvai at Monte San Nicola is older than expected. Based on the biostratigraphy developed for the Mediterranean area, this geomagnetic event should be approximated by the biohorizon Top *D. brouweri* at ca. 1.95 Ma (Raffi et al., 2006), slightly younger than the Base common *G. truncatulinoides truncatulinoides* (2.00 Ma; Lirer et al., 2019). In our section (Figs. 6 and 7), the base of the Olduvai seems to precede both these events, as it occurs some 10 m below the expected position according to our calculations. This pattern is similar to that reported by Channell et al. (1992) for the “Type” section, where the base of the Olduvai was preceded by a long interval of undetermined magnetic polarity.

The short normal polarity interval straddling sapropel B2, between the Gauss/Matuyama and the base of the Olduvai (R1.n1; Fig. 7), may correlate to the Reunion normal Chron C2r.1n. However, its stratigraphic position is not in keeping with that found at the coeval Singa section, where it occurs in correspondence to sapropel B5 (Zijderveld et al., 1991). According to our age model, interval R1.n1 extends from ca. 2.215 to 2.255 Ma, corresponding to a duration of ca. 40 kyr, in general agreement with the age and duration calculated for this subchron in lava flows and marine sediments (e.g., Channell et al., 2003, 2020; Singer et al., 2014). Still, the lack of correlation to the paleomagnetic record reconstructed for the Singa section suggests that further dedicated investigations are needed before validating the correlation of this subchron to the Reunion.

Paleomagnetic properties of sediments offer consistent results in the uppermost part of the section. In particular, the top of the Olduvai is documented convincingly at ca. 81.5 m, ca. 3 m above the biohorizon Base common *G. pachyderma* and ca. 2 m below sapropel layer *f* (Figs. 6 and 7). Based on the sediment accumulation rates calculated for this part of the stratigraphy, we obtained an age of ca. 1.78 Ma for this paleomagnetic event, in close agreement with that proposed by Lepre and Kent (2010) and other authors (e.g., Gradstein et al., 2020; Channell et al., 2020).

3.5. Astronomical tuning and chronology

The logical sedimentary cyclicity shown by many deep-marine Pliocene and Lower Pleistocene sections from Southern Italy and Sicily can be interpreted as the lithological response of the Mediterranean Basin to orbitally-driven climatic variability (e.g., Lourens et al., 2004, and references within). Many of these sections were subjected to astronomical tuning, i.e., the process of correlating physical stratigraphic signals to astronomical target curves such as precession, obliquity, eccentricity and insolation, which allowed for the construction of the Astronomical Tuned Neogene Time Scale (ATNTS 2004; Lourens et al., 2004). One of the main guidelines is the assumption that deposition of Mediterranean sapropel layers (either “true”, “failed” or “missing”, in the sense used in this paper)

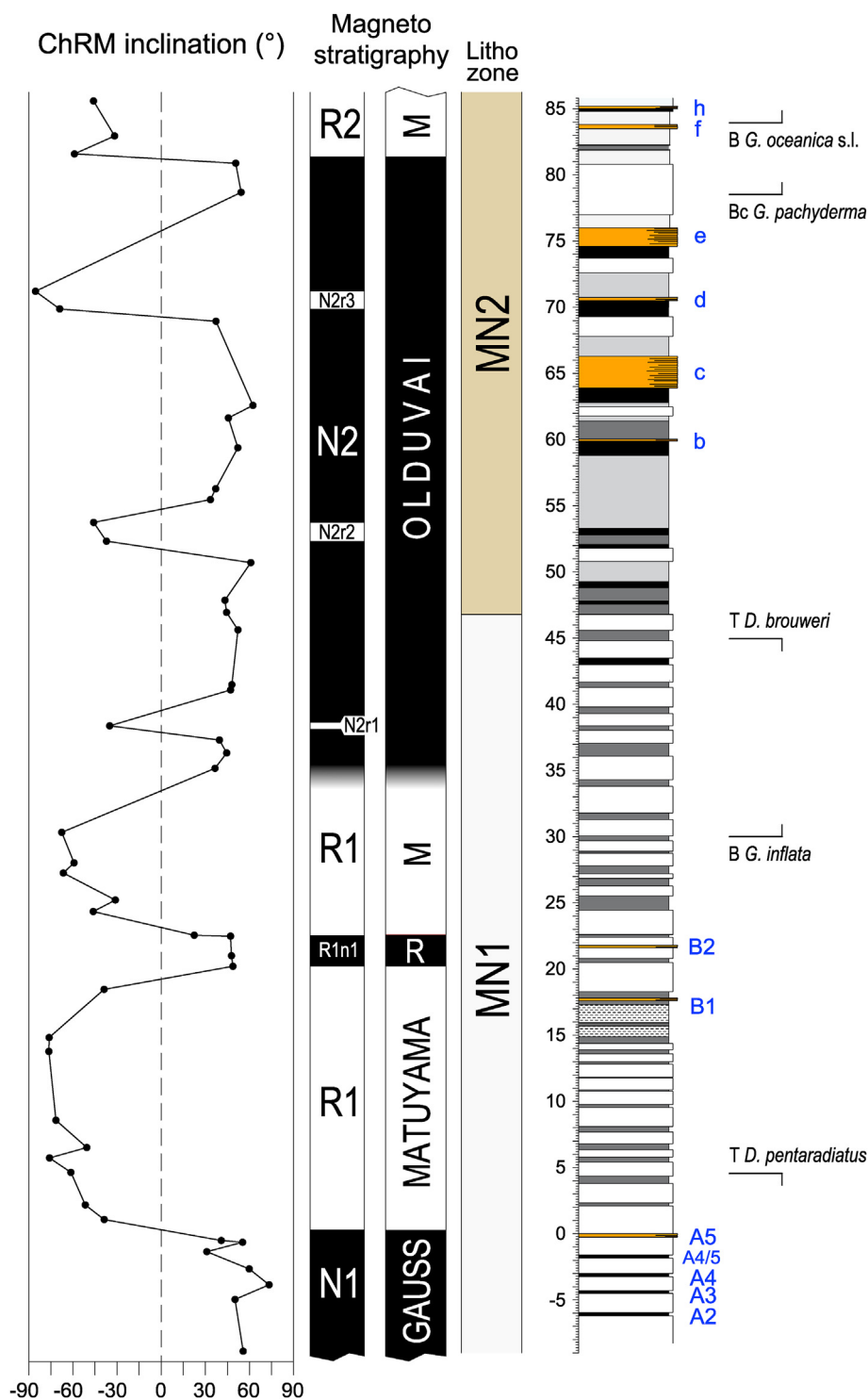


Fig. 7. Results of the paleomagnetic investigation in the “Mandorlo” section. Left: ChRM inclination values, calculated for the samples that yielded a dependable paleomagnetic result. Centre: magnetostratigraphic interpretation, with indication of Chrons formal coding (left column) and names (right). R: Reunion. Chron boundaries have been defined in correspondence to the midpoints of polarity transits, i.e., inclination = 0°. The potential Reunion Subchron (R1n1) and the short-lived intervals of reverse polarity within the Olduvai Subchron (N2r1-N2r3) have been graphically restricted to the intervals where the relative samples are located. The stratigraphic position of relevant biohorizons is also reported (far right).

was triggered by insolation maxima (e.g., Hilgen, 1999; Lourens et al., 1996). Following this criterion, we attempted establishing an astronomical tuning of the “Mandorlo” section, as reported in Fig. 8. The sapropel layers of cluster A (even-numbered i-cycles 258 to 250), as well as the laminated layers of clusters B (i-cycles 222

and 216) and C (even-numbered i-cycles 182 to 176, 170 and 168), were employed as landmarks following the chronology of Lourens et al. (1996). Only two weak insolation maxima seem to be lithologically not expressed on our log (Fig. 8). Although this may represent a genuine signal, we stress that the physical stratigraphic

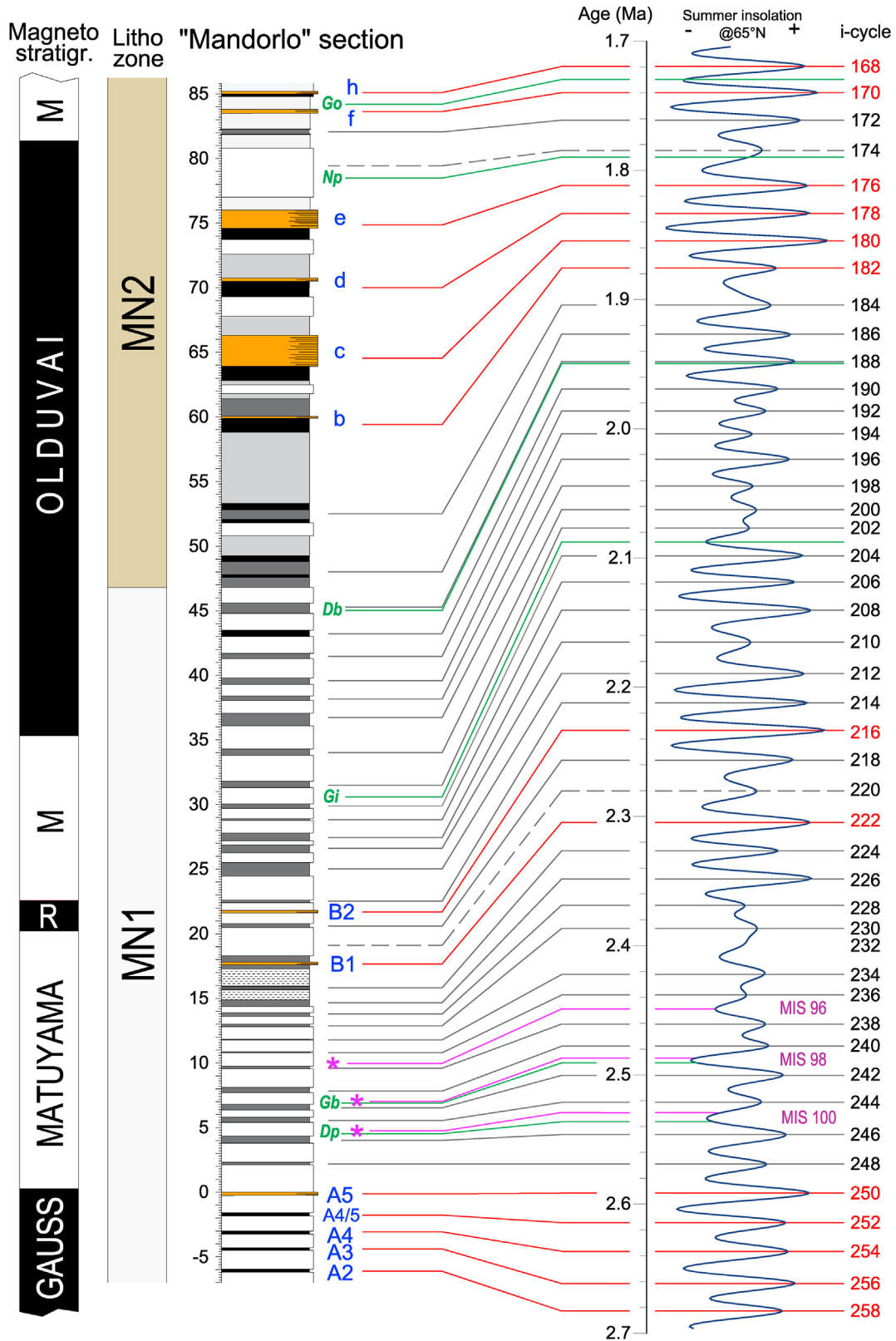


Fig. 8. Astronomical tuning of the "Mandorlo" section based on a visual bed-to-peak correlation (continuous grey lines). Target curve is the average summer insolation (June) at 65°N according to the La04 orbital solution of Laskar et al. (2004). Red lines indicate sapropel-to-peak correlations after Hilgen (1991a,b), Lourens et al. (1996) and Becker et al. (2005). Dashed lines indicate insolation peaks that has no lithological match in our stratigraphic log (see text for discussion). Green lines and labels indicate stratigraphically significant biohorizons. Dp: Top *Discoaster pentaradiatus*. Gb: Top common *Globorotalia bononiensis*. Gi: Base *Globorotalia inflata*. Db: Top *Discoaster broweri*. Np: Base common *Neogloboquadrina pachyderma*. Go: Base *Gephyrocapsa oceanica*. Purple asterisks and lines indicate the stratigraphic position of the influxes of *Neogloboquadrina atlantica atlantica* correlative to the glacial MIS 100, 98 and 96 (Becker et al., 2005). (For interpretation of the references to color in this figure legend, the reader is referred to the Web version of this article.)

investigation is subjective and may depend on exposure and weather conditions. Since our lithological description was unbiased, we cannot exclude that few thin and flimsy dark clayey layers may have gone unnoticed.

Further control points were provided by the three short-lived influxes of *N. atlantica atlantica* (red asterisks between 3 and 12 m in Fig. 6), which correlate to the glacial intervals of MIS 100, 98 and 96 (i-cycles 245, 241 and 237, respectively; e.g., Lourens et al., 1996; Becker et al., 2005). The general agreement between peaks in the insolation curve and lithological cycles is also confirmed by the consistent position of major biohorizons with respect to the ATNTS, as indicated in Fig. 6 and Table 1. We are thus confident that the “Mandorlo” section offers a complete and virtually continuous record of the Gelasian Stage, including the top of the underlying Piacenzian and the bottom of the Calabrian Stage above. The duration of possible stratigraphic gaps within, if any, is shorter than half a precession cycle, thus negligible at the available time resolution and detail.

Based on the constraints provided by standard biostratigraphic events, previously validated by the astronomical tuning, as well as remarkable astrochronological tie points, we developed an age/depth plot as reported in Table 1 and shown in Fig. 9. As discussed above, our paleomagnetic record does not provide unequivocal information for some of the recognized reversals, that will need to be addressed by means of further investigations. Therefore, for the time being, we decided not to employ polarity ages in our age/depth model. The calculated sedimentation rates (Table 1) range from ca. 4 to ca. 25 cm/kyr, ca. 14 cm/kyr on average, in keeping with estimates from central Mediterranean slope to outer-shelf settings over the Middle-Late Quaternary (Incarbona et al., 2009; Toucanne et al., 2011; Capraro et al., 2011, 2017). Sediment accumulation rates remain steadily below the 10 cm/kyr threshold from the bottom of the section up to ca. 30 m. From here, a sharp but gradual increase can be observed (Fig. 9). Deposition of the very expanded laminites *c* and *e* (Figs. 5 and 6) confirms that the terrigenous input to the basin increased considerably in this stratigraphic interval, as further emphasized by the concomitant change in sediment color and competence (see above). In the upper part of the section sediment accumulation rates decrease again, still remaining higher than those documented in the lower Gelasian

interval. According to our age model, the major increase in sedimentation rates in the “Mandorlo” section begun at ca. 2.1 Ma, close to the ‘first deep glaciation’ and the abrupt events of glaciation-related sea-level drop (Rohling et al., 2014). Therefore, superimposed on unpredictable regional changes in sediment supply, the increase in sediment accumulation rates immediately prior to the Gelasian/Calabrian boundary may reflect a period of increased yield of terrigenous and aeolian material to the central Mediterranean area in response to major changes in the global climate regimes.

In Fig. 10, we report on the correlation between the “Mandorlo” section (here referred to as “Monte San Nicola”) and other coeval key sections from the central Mediterranean area. These are represented not only by sections laid in the same Caltanissetta basin as Monte San Nicola, such as Punta Piccola (Castradori et al., 1998), but also successions from the Ionian Calabria (Southern Italy), such as the Vrica (Selli et al., 1977) and Singa sections (Zijderveld et al., 1991), or even from northern Italy, such as the Marecchia valley (Rio et al., 1997a). This long-distance, yet extremely detailed, correlation is provided by several criteria, among which are the marine biostratigraphy based on calcareous plankton, paleomagnetic data, the sapropel record, and henceforth the astronomical tuning of the entire Gelasian succession. This paper provides substantial advances in our knowledge of the Monte San Nicola section that will further improve the small-scale detail and correlatability of the local succession at both the regional and global scales. In particular, we increased dramatically the biomagnetostratigraphic detail across the GSSP of the Gelasian Stage (Rio et al., 1998) and especially in the stratigraphy above, which was hitherto well documented only in the interval corresponding to MIS 100 (Becker et al., 2005).

3.6. The Monte San Nicola section as unit-Stratotype of the Gelasian Stage

Present-day procedures for formally defining lower-rank chronostratigraphic units, i.e. Stages, consist in establishing Boundary Stratotypes (GSSPs; Hedberg, 1976). As a GSSP only defines the bottom of a particular Stage, its upper boundary is implicitly marked by the GSSP of that immediately above. GSSPs may even be defined in short and disjointed sections, regardless of the

Table 1
Bio- and chronostratigraphic events employed for reconstructing the age-depth plot reported in Fig. 9.

| Event | Level (m) | Age (Ma) | Sed. rate (cm/kyr) | Rank | Reference |
|-----------------------------------|-----------|----------|--------------------|-----------------|-----------------------|
| BASE <i>G. oceanica</i> s.l. | 84.2 | 1.730 | | standard | Raffi et al. (2006) |
| BASE COMMON <i>N. pachyderma</i> | 78.6 | 1.790 | 9.3 | standard | Lirer et al. (2019) |
| Gelasian/Calabrian boundary | 76 | 1.806 | 16.3 | astrochronology | Lourens et al. (1996) |
| Sapropel d (midpoint) | 70.6 | 1.829 | 23.5 | astrochronology | Lourens et al. (1996) |
| Sapropel c (midpoint) | 65.2 | 1.851 | 24.5 | astrochronology | Lourens et al. (1996) |
| Sapropel b (midpoint) | 60 | 1.872 | 24.8 | astrochronology | Lourens et al. (1996) |
| TOP <i>D. triradiatus/broweri</i> | 45 | 1.950 | 19.2 | standard | Backman et al. (2012) |
| BASE <i>G. inflata</i> | 30 | 2.090 | 10.7 | standard | Lirer et al. (2019) |
| TOP COMMON <i>G. bononiensis</i> | 6.9 | 2.450 | 6.4 | standard | Lirer et al. (2019) |
| TOP <i>D. pentaradiatus</i> | 4.6 | 2.512 | 3.7 | standard | Backman et al. (2012) |
| Piacenzian/Gelasian boundary | 0 | 2.581 | 6.7 | astrochronology | Rio et al. (1998) |
| Sapropel A2 | -6 | 2.679 | 6.1 | astrochronology | Lourens et al. (1996) |

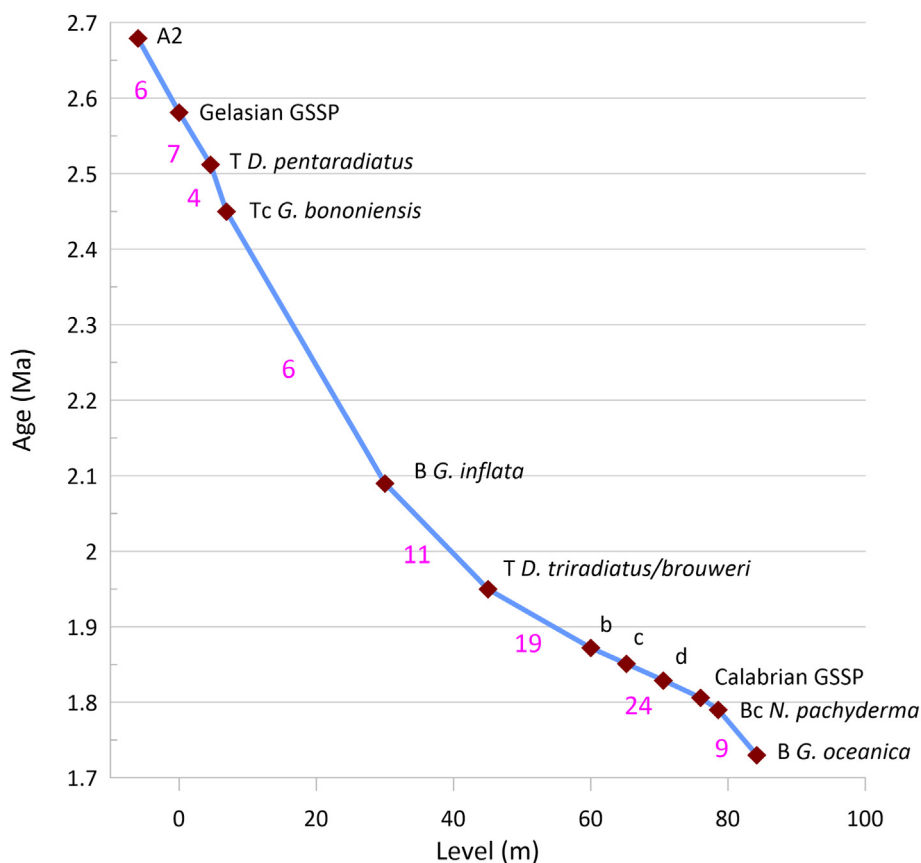


Fig. 9. Age-depth plot based on the main bio- and chronostratigraphic events recognized in the “Mandorlo” section. Ages of the considered events and corresponding levels in the local stratigraphy are reported in Table 1. A2 indicates the lowermost sapropel found in the “Mandorlo” section. Letters b, c, d indicate the midpoints of the homonymous sapropel layers at Vrica (Selli et al., 1977). Numbers in purple indicate the average sediment accumulation rates (as cm/kyr) in the interval of relevance. (For interpretation of the references to color in this figure legend, the reader is referred to the Web version of this article.)

stratigraphy above and below, assuming that they prove continuous and complete in the interval containing the relevant markers for boundary recognition. The enforcing of “topless” Stages addresses the need to define formal chronostratigraphic units even in the absence of sections fully and continuously covering the relevant stratigraphic interval, the latter being the exception rather than the general rule.

These chronostratigraphic practices emphasize the importance of unit boundaries, rather than their content. Indeed, Stages defined by GSSPs only may be considered as “empty boxes” because, in their definition, age control and correlation are not demanded (and, therefore, not necessarily existing) in the stratigraphy above the boundary, which actually constitutes the unit body.

Part of the scientific community believes that chronostratigraphy would benefit from the formalization of sedimentary successions that host both the complete body of rock and the upper and lower boundaries of individual Stages in one and the same section, i.e., Unit Stratotypes (Gradstein et al., 2020). Following the preconception that no section can actually offer a truly continuous stratigraphic record (Hedberg, 1976; Walsh et al., 2004), opponents of this proposal generally argue that the number of sections suitable as Units Stratotypes is too small to justify the effort, and this would eventually result in an unbalanced chronostratigraphic time scale.

Recently, Hilgen et al. (2020) published a formal proposal to introduce a new chronostratigraphic concept beyond the “traditional” Unit Stratotype, which is the Astronomical Unit Stratotype (AUS). As basic requirement, candidate AUS sections should be

represented by cyclical deep-marine successions amenable to astronomical tuning, which would prove the completeness of the succession and, most importantly, provide accurate age control for each and any of the depositional events within. In the process, individual cycles used for tuning may be formally defined as chronozones, i.e. chronostratigraphic units of lower rank than the Stage (Hilgen et al., 2006). Compared to the bare Unit Stratotypes, AUSs would minimize the risk of harboring incomplete and/or non-continuous stratigraphic records and, with respect to the sole GSSPs, they would secure major improvements both in terms of age control and correlation potential of the unit body. Implementing this approach for the cyclical deep-marine Cenozoic successions that are beautifully exposed along the coasts of the circum-Mediterranean area would be effortless. In particular, based on the high-resolution biomagnetostratigraphic investigations and astronomical tuning performed in the last decades (e.g., Hilgen, 1991b; Lourens et al., 1996), sections from Southern Italy and Sicily have been demonstrated to cover completely and continuously the Pliocene and Lower Pleistocene interval, and may therefore serve as AUSs of the Stages within.

Our astronomical tuning of the “Mandorlo” section (Fig. 8), to be further validated, demonstrates for the first time that the Monte San Nicola succession preserves a complete and virtually continuous record of the entire Gelasian Stage. We believe that, if the concept of AUS will be formally accepted (see Hilgen et al., 2006, 2020, for discussion on the pros and cons of the proposal), the Monte San Nicola succession – the “Mandorlo” section in particular – will serve perfectly as the reference section for both the Gelasian

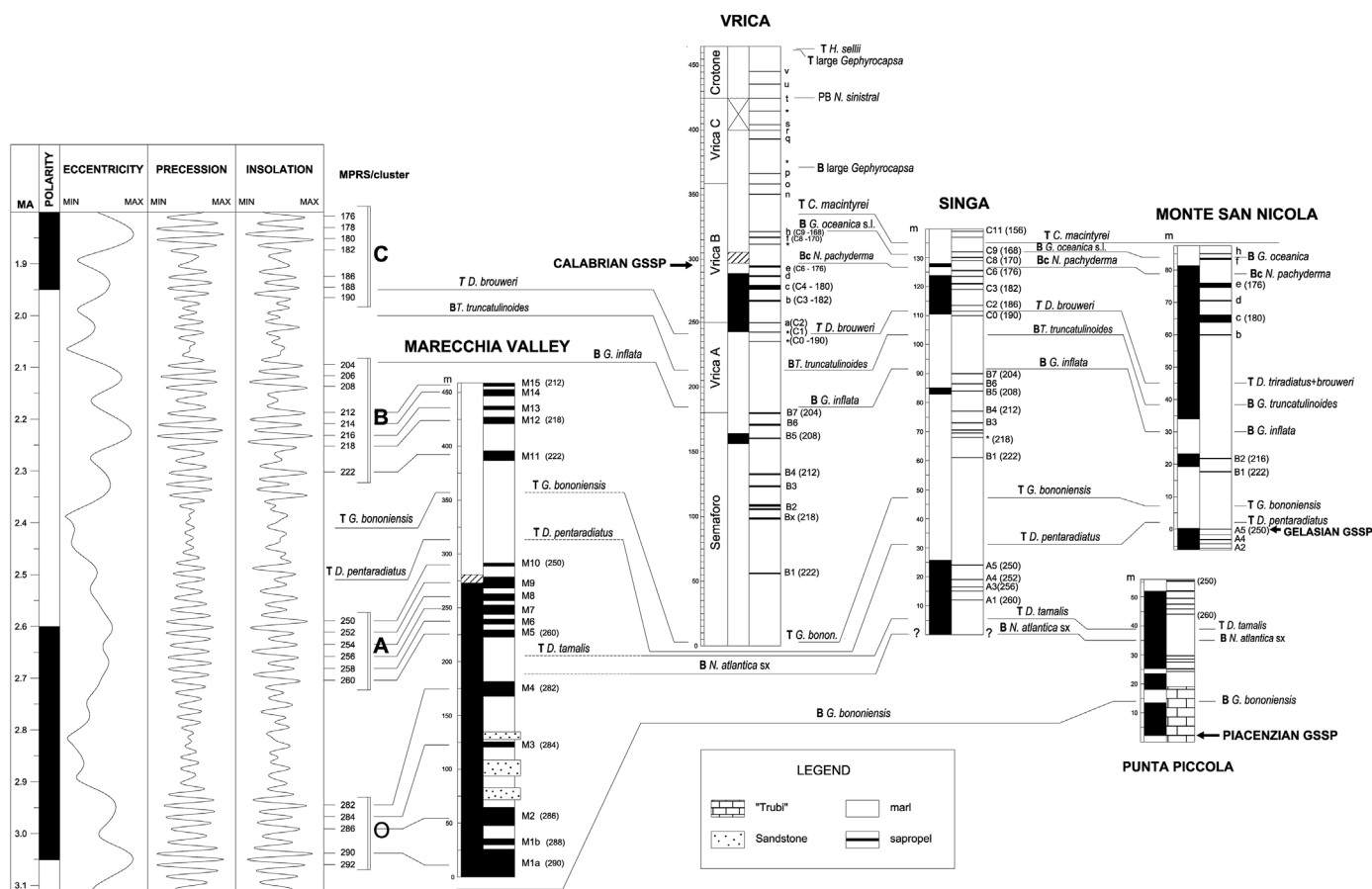


Fig. 10. Biomagnetostratigraphic correlation of the “Mandorlo” section (reported here as “Monte San Nicola”) with other coeval, sapropel-bearing reference sections in northern Italy (Marecchia Valley), southern Italy (Singa, Vrica) and Sicily (Punta Piccola). Correlation between the sections is provided by key biohorizons and MPRS layers of clusters O/M, A, B, C. Precession cycles (i-cycles) are also indicated in brackets. Individual sapropel layers are linked to the astronomical target curves (eccentricity, precession, and summer insolation at 65°N) calculated from the La04 orbital solution of Laskar et al. (2004). Data for the Singa and Punta Piccola sections are from Hilgen (1991a). Data for the Vrica section are from Lourens et al. (1996). Data for the Marecchia Valley are from Rio et al. (1997a).

GSSP and its AUS.

4. Conclusions

The new suite of physical- and chronostratigraphic constraints presented in this paper has been obtained via an updated study of the upper Piacenzian-lower Calabrian succession of Monte San Nicola (Gela, Southern Sicily), where the GSSP of the Gelasian Stage was established (Rio et al., 1998). Detailed biostratigraphic and paleomagnetic analyses, in addition to a careful physical stratigraphic investigation, have been performed from scratch on two sections in the Monte San Nicola badlands, namely the “Type” and the “Mandorlo” sections. Our results indicate that the two sections encompass the entire Gelasian Stage, as they contain both the Piacenzian/Gelasian and Gelasian/Calabrian boundaries.

We confirm that the Piacenzian/Gelasian boundary is approximated closely by the biohorizons Top *D. pentaradiatus*, Top common *N. atlantica* and Top common *G. bononiensis* as well as the Gauss/Matuyama geomagnetic reversal, in agreement with the original definition of Rio et al. (1998). The Gelasian/Calabrian boundary is marked by the distinctive succession of sapropel layers c to h, as first defined in the reference section of Vrica (Pasini and Colalongo, 1997; Raffi and Thunell, 1996). The Base *G. oceanica s.l.* and Base common *G. pachyderma* biohorizons represent the main biostratigraphic proxies of the boundary, that also occurs very close to the top of the Olduvai Subchron. The intervening stratigraphy

provides a series of bioevents that is in good agreement with the reference biostratigraphy validated for the central Mediterranean region (Raffi et al., 2006; Lirer et al., 2019).

Altogether, our data confirm that the “Mandorlo” section hosts a complete and undisturbed record of the entire Gelasian Stage. In contrast, physical stratigraphic evidences obtained for the “Type” section suggest that a short segment of this “historical” section is affected by poor exposure conditions and faulting, which puts in question its fitness to serve as Unit Stratotype for the Gelasian Stage. However, it must be stressed that the problems affecting the “Type” section occur well above the stratigraphic interval where the Piacenzian/Gelasian boundary is located. The Gelasian GSSP, as presently defined, is therefore pristine and should not be put in question. We conclude that the “Mandorlo” section holds all the basic requirements for hosting the Astronomical Unit Stratotype of the Gelasian Stage, as the whole interval of relevance is there represented by a continuous, fossiliferous and undisturbed stratigraphic record that is demonstrated to correlate seamlessly to the main Mediterranean reference sections, and beyond.

Declaration of Competing Interest

The authors declare that they have no known competing financial interests or personal relationships that could have appeared to influence the work reported in this paper.

Acknowledgments

We are grateful to Frits Hilgen and an anonymous Reviewer for providing valuable suggestions and recommendations that greatly helped improve the manuscript. This research was funded by DOR (ex 60%, University of Padova) to L.C. and D.R.

References

- Backman, J., Shackleton, N.J., 1983. Quantitative biochronology of Pliocene and early Pleistocene calcareous nannoplankton from the atlantic Indian and pacific oceans. *Mar. Micropaleontol.* 8, 141–170. [https://doi.org/10.1016/0377-8398\(83\)90009-9](https://doi.org/10.1016/0377-8398(83)90009-9).
- Backman, J., Pestiaux, P., 1987. Pliocene discoaster abundance variations, deep sea drilling project site 606: biochronology and paleoenvironmental implications. In: Ruddiman, W.F., Kidd, R.B., Thomas, E., et al. (Eds.), *Init. Repts. DSDP*, 94. U.S. Govt. Printing Office, Washington, pp. 903–910. <https://doi.org/10.2973/dsdp.proc.94.126.1987>.
- Backman, J., Raffi, I., Rio, D., Fornaciari, E., Palike, H., 2012. Biozonation and biochronology of Miocene through Pleistocene calcareous nannofossils from low and middle latitudes. *Newsl. Stratigr.* 45, 221–244. <https://doi.org/10.1127/0078-0421/2012/0022>.
- Barbieri, F., 1967. The foraminifera in the Pliocene section vernasca Castell'Arquato including the "piacenzian stratotype". *Soc. It. Sc. Nat. Mus. Civ. Sc. Nat. Milano, Mem.* 15, 145–163.
- Becker, J., Lourens, L.J., Hilgen, F.J., van der Laan, E., Kouwenhoven, T.J., Reichert, G.-J., 2005. Late Pliocene climate variability on Milankovitch to millennial time scales: a high-resolution study of MIS100 from the Mediterranean. *Palaeogeogr. Palaeoclimatol. Palaeoecol.* 228, 338–360.
- Beneo, E., 1958. Sull'olistostroma quaternario di Gela (Sicilia meridionale). *Boll. Serv. Geol. d'It.* 79, 5–15.
- Berggren, W.A., Kent, D.V., Flynn, J.J., Van Couvering, J.A., 1985. Cenozoic geochronology. *Geol. Soc. Am. Bull.* 96 (11), 1407–1418.
- Bertoldi, R., Rio, D., Thunell, R., 1989. Pliocene-Pleistocene vegetational and climatic evolution of the south-central Mediterranean: *Palaeogeogr. Palaeoclimatol. Palaeoecol.* 72, 263–275.
- Bolli, H.M., Saunders, J.B., 1985. Oligocene to Holocene low latitude planktic foraminifera. In: Bolli, H.M., Saunders, J.B., Perch-Nielsen, K. (Eds.), *Plankton Stratigraphy. Volume 1: Planktic Foraminifera, Calcareous Nannofossils and Calpionellids*. Cambridge University Press, pp. 155–262.
- Bonaduce, G., Sprovieri, R., 1984. The appearance of *Cytheropteron testudo* Sars (Crustacea: ostracoda) is a Pliocene event. Evidences from a Sicilian sequence (Italy). *Boll. Soc. Paleontol. Ital.* 23 (1), 131–136.
- Brocchi, G., 1814. *Conchiologia fossile subapennina, con osservazioni geologiche sugli Apennini e sul suolo adiacente*, vol. 1. Stamperia reale, p. 712.
- Bromley, R.G., Ekdale, A.A., 1984. *Chondrites*: a trace fossil indicator of anoxia in sediments. *Science* 224, 872–874.
- Cande, S.C., Kent, D.V., 1995. Revised calibration of the geomagnetic polarity time scale for the late Cretaceous and Cenozoic. *J. Geophys. Res. C Oceans Atmos.* 100, 6093–6095.
- Capraro, L., Massari, F., Rio, D., Fornaciari, E., Backman, J., Channell, J.E.T., Macri, P., Prosser, G., Speranza, F., 2011. Chronology of the lower-middle Pleistocene succession of the south-western part of the Crotona Basin (Calabria, southern Italy). *Quat. Sci. Rev.* 30, 1185–1200.
- Capraro, L., Ferretti, P., Macri, P., Scarponi, D., Tateo, F., Fornaciari, E., Bellini, G., Dalan, G., 2017. The valle di Manche section (Calabria, southern Italy): a high-resolution record of the early-middle Pleistocene transition (MIS 21–MIS 19) in the central mediterranean. *Quat. Sci. Rev.* 165, 31–48.
- Caruso, A., 2004. Climatic changes during late Pliocene and early Pleistocene at Capo Rossello (sicily, Italy): response from planktonic foraminifera. In: Coccioni, R., et al. (Eds.), *Proc. 1st Italian Meeting on Environmental Micropaleontology*, vol. 9. Grzybowski Foundation Special Publication, pp. 17–36.
- Castradori, D., Rio, D., Hilgen, F.J., Lourens, L.J., 1998. The global standard stratotype-section and point (GSSP) of the Piacenzian Stage (Middle Pliocene). *Episodes* 21, 88–93.
- Catalano, R., Channell, J.E.T., D'Argenio, B., Napoleone, G., 1977. Mesozoic paleogeography of the southern Apennines and Sicily. *Problems of paleotectonics and paleomagnetism. Mem. Soc. Geol. Ital.* 15, 95–118, 1977.
- Catalano, R., Valenti, V., Albanese, C., Accaino, F., Sulli, A., Tinivella, U., Giustiniani, M., 2013. Sicily's fold—thrust belt and slab roll-back: the SI.RI.PRO seismic-crustal transect. *J. Geol. Soc.* 170, 451–464. <https://doi.org/10.1144/jgs2012-099>.
- Channell, J.E.T., Rio, D., Sprovieri, R., Glaçon, G., 1990. Biomagnetostratigraphic correlations from leg 107 in the tyrrhenian sea. In: Kastens, K.A., Mascle, J., et al. (Eds.), *Proc. ODP, Sci. Results*, vol. 107. Ocean Drilling Program, College Station, TX, pp. 669–682. <https://doi.org/10.2973/odp.proc.sr.107.180.1990>.
- Channell, J.E.T., Di Stefano, E., Sprovieri, R., 1992. Calcareous plankton biostratigraphy, magnetostratigraphy and paleoclimatic history of the plio-pleistocene Monte San Nicola section (southern sicily). *Boll. Soc. Paleont. It.* 31, 351–382.
- Channell, J.E.T., Lubs, J., Raymo, M.E., 2003. The Réunion subchronone at ODP site 981 (Feni drift, North Atlantic). *Earth Planet Sci. Lett.* 215, 1–12.
- Channell, J.E.T., Singer, B.S., Jichab, B.R., 2020. Timing of Quaternary geomagnetic reversals and excursions in volcanic and sedimentary archives. *Quat. Sci. Rev.* 228, 106114.
- Cita, M.B., 1975. Planktonic foraminiferal biozonation of the Mediterranean Pliocene deep-sea record. A revision. *Riv. Ital. Paleontol. Stratigr.* 81, 527–544.
- Cita, M.B., 1973. Pliocene stratigraphy and chronostratigraphy. In: Ryan, W.B.F., Hsu, K.J., et al. (Eds.), *Init. Rep. Of the DSDP*, vol. 13, pp. 1343–1379.
- Cita, M.B., Gartner, S., 1973. The stratotype Zanclean foraminiferal and nannofossil biostratigraphy. *Riv. Ital. Paleontol.* 79 (4), 503–558.
- Cita, M.B., Capraro, L., Ciaranfi, N., Di Stefano, E., Lirer, F., Maiorano, P., Marino, M., Raffi, I., Rio, D., Sprovieri, R., Stefanelli, S., Vai, G.B., 2008. The Calabrian stage redefined. *Episodes* 31 (4), 408–419.
- Cita, M.B., Gibbard, P.L., Head, M.J., 2012. The ICS Subcommittee on quaternary stratigraphy, 2012. Formal ratification of the GSSP for the base of the Calabrian stage GSSP (Pleistocene series, quaternary system). *Episodes* 35, 388–397.
- Dansgaard, W., Johnsen, S.J., Clausen, H.B., Dahl-Jensen, D., Gundestrup, N.S., Hammer, C.U., Hvidberg, C.S., Steffensen, J.P., Sveinbjornsdottir, A.E., Jouzel, J., 1993. Evidence for general instability of past climate from a 250-kyr ice-core record. *Nature* 364, 218–220.
- De Kaenel, E., Siesser, W.G., Murat, A., 1999. Pleistocene calcareous nannofossil biostratigraphy and the western Mediterranean sapropels, Sites 974 to 977 and 979. In: Zahn, R., Comas, M.C., Klaus, A. (Eds.), *Proc. ODP, Sci. Results*, vol. 161. Ocean Drilling Program, College Station, TX, pp. 159–183. <https://doi.org/10.2973/odp.proc.sr.161.250.1999>.
- De Visser, J.P., Ebbing, J.H.J., Gudjonsson, L., Hilgen, F.J., Jorissen, F.J., Verhallen, P.J.J.M., Zevenboom, D., 1989. The origin of rhythmic bedding in the Pliocene Trubi Formation of Sicily, southern Italy. *Palaeogeogr. Palaeoclimatol. Palaeoecol.* 69, 45–66.
- Di Grande, A., Giandinoto, V., 2002. Plio-Pleistocene Sedimentary Facies and Their Evolution in Centre-Southeastern Sicily: a Working Hypothesis. *European Geosciences Union (Stephan Mueller Special Publication Series)*, pp. 211–221.
- Di Stefano, E., 1998. Calcareous nannofossil quantitative biostratigraphy of holes 969E and 963B (eastern mediterranean). In: Robertson, A.H.F., Emeis, K.-C., Richter, C., Camerlenghi, A. (Eds.), *Proc. ODP, Sci. Results*, vol. 160. Ocean Drilling Program, College Station, TX, pp. 99–112. <https://doi.org/10.2973/odp.proc.sr.160.009.1998>.
- Di Stefano, E., Sprovieri, R., Caruso, A., 1993. High resolution biochronology in the Monte Narbone formation of the Capo Rossello section and the mediterranean first occurrence of *Globorotalia truncatulinoides*. *Riv. Ital. Paleontol. Stratigr.* 99, 357–370.
- Driever, B.W.M., 1984. The terminal record of *Discoaster* in the Mediterranean and in the Atlantic DSDP site 397, and the Pliocene-Pleistocene boundary. *Kon. Ned. Akad. Wetensch. Proc., Ser. B* 87, 77–102.
- Driever, B.W.M., 1988. Calcareous nannofossil biostratigraphy and paleoenvironmental interpretation of the Mediterranean Pliocene. *Utrecht Micropaleontol. Bull.* 36, 245.
- Florindo, F., Sagnotti, L., 1996. Revised magnetostratigraphy and rock magnetism of Pliocene sediments from valle ricca (Rome, Italy). *Geological Society, London, Special Publications* 105, 219–223. <https://doi.org/10.1144/GSL.SP.1996.105.01.20>.
- Gardin, S., Monechi, S., 1998. Palaeoecological change in the middle to low latitude calcareous nannoplankton at the Cretaceous/Tertiary boundary. *Bull. Soc. Geol. Fr.* 5, 709–723.
- Gasparo Morticelli, M., Valenti, V., Catalano, R., Sulli, A., Agate, M., Avellone, G., Albanese, C., Basilone, L., Gugliotta, C., 2015. Deep controls on foreland basin system evolution along the Sicilian fold and thrust belt. *Bull. Soc. Geol. Fr.* 186 (4–5), 273–290.
- Ghisetti, F., Gorman, A.R., Grasso, M., Vezzani, L., 2009. Imprint of foreland structure on the deformation of a thrust sheet: the Plio-Pleistocene Gela Nappe (southern Sicily, Italy). *Tectonics* 28, TC4015. <https://doi.org/10.1029/2008TC002385>.
- Gibbard, P.L., Head, M.J., Walker, M.J., 2010. Subcommittee on quaternary stratigraphy. Formal ratification of the quaternary System/Period and the Pleistocene series/epoch with a base at 2.58 Ma. *J. Quat. Sci.* 25 (2), 96–102.
- Gibbard, P.L., Head, M.J., 2010. The newly-ratified definition of the Quaternary System/Period and redefinition of the Pleistocene Series/Epoch, and comparison of proposals advanced prior to formal ratification. *Episodes* 33, 152–158.
- Glaçon, G., Rio, D., Sprovieri, R., 1990a. Calcareous plankton pliocene-pleistocene biostratigraphy in the tyrrhenian sea (western mediterranean, leg 107). In: Kastens, K.A., Mascle, J., et al. (Eds.), *Proc. ODP, Sci. Results*, vol. 107. Ocean Drilling Program, College Station, TX, pp. 683–693.
- Glaçon, G., Vergnaud-Grazzini, C., Iaccarino, S., Rehault, J.P., Randrianasolo, A., Sierro, F.J., Weaver, P., 1990b. Planktonic foraminiferal events and stable isotopic record in the upper Miocene of the tyrrhenian sea, ODP site 654, leg 107. In: Kastens, K.A., Mascle, J., et al. (Eds.), *Proc. ODP, Sci. Results*, vol. 107. Ocean Drilling Program, College Station, TX, pp. 415–427.
- Gradstein, F.M., Ogg, J.G., Schmitz, M.D., Ogg, G.M., 2020. *The Geological Time Scale 2020*. Elsevier, Amsterdam, Netherlands. <https://doi.org/10.1016/C2020-1-02369-3>.
- Grasso, M., Manzoni, M., Quintili, A., 1987. Misure magnetiche sui Trubi Fm. infra-pliocenicici della Sicilia orientale: possibili implicazioni stratigrafiche e strutturali. *Mem. Soc. Geol. It.* 38, 459–474.
- Hedberg, H.D. (Ed.), 1976. *International Stratigraphic Guide*. Wiley, New York, p. 200.
- Heinrich, H., 1988. Origin and consequences of cycling ice rafting in the Northeast Atlantic Ocean during the past 130,000 years. *Quat. Res.* 29, 143–152.
- Hemleben, C., Spindler, M., Anderson, O.R., 1989. *Modern Planktonic Foraminifera*.

- Springer New York, New York, NY. <https://doi.org/10.1007/978-1-4612-3544-6>.
- Herbert, T.D., Ng, D., Cleaveland Peterson, L., 2015. Evolution of Mediterranean Sea surface temperatures 3.5–1.5 Ma: regional and hemispheric influences. *Earth Planet Sci. Lett.* 409, 307–318.
- Hilgen, F.J., 1991a. Astronomical calibration of Gauss to Matuyama sapropels in the Mediterranean and implication for the geomagnetic polarity time scale. *Earth Planet Sci. Lett.* 104, 226–244. [https://doi.org/10.1016/0012-821X\(91\)90206-W](https://doi.org/10.1016/0012-821X(91)90206-W).
- Hilgen, F.J., 1991b. Extension of the astronomically calibrated (polarity) time scale to the Miocene/Pliocene boundary. *Earth Planet Sci. Lett.* 107, 349–368. [https://doi.org/10.1016/0012-821X\(91\)90082-S](https://doi.org/10.1016/0012-821X(91)90082-S).
- Hilgen, F.J., Abdul Aziz, H., Krijgsman, W., Langereis, C.G., Lourens, L.J., Meulenkamp, J.E., Raffi, I., Steenbrink, J., Turco, E., van Vugt, N., Wijbrans, J.R., Zachariasse, W.J., 1999. Present status of the astronomical (polarity) time-scale for the Mediterranean Late Neogene. *Philos. Trans. R. Soc. London, Ser. A: Mathematical, Physical and Engineering Sciences* 357 (1757), 1931–1947.
- Hilgen, F.J., Brinkhuis, H., Zachariasse, W.J., 2006. Unit stratotypes for global stages: the Neogene perspective. *Earth Sci. Rev.* 74, 113–123.
- Hilgen, F.J., Lourens, L., Pälike, H., research support team, 2020. Should Unit-Stratotypes and Astrochronozones be formally defined? A dual proposal (including postscriptum). *News. Stratigr.* 53, 19–39.
- Howell, M.W., Thunell, R., Tappa, E., Rio, D., Sprovieri, R., 1988. Late Neogene laminated and opal-rich facies from the Mediterranean region: geochemical evidence for mechanisms of formation. *Palaeogeogr. Palaeoclimatol. Palaeoecol.* 64 (3–4), 265–286.
- Incarbona, A., Di Stefano, E., Bonomo, S., 2009. Calcareous nannofossil biostratigraphy of the central Mediterranean Basin during the last 430,000 years. *Stratigraphy* 6 (1), 33–34.
- Istituto Nazionale di Geofisica e Vulcanologia (INGV), 2001. Italian Magnetic Network and Geomagnetic field maps of Italy at year 2000.0. *Boll. Geod. Sci. Affini* 60, 261–291.
- Laj, C., Channell, J.E.T., 2007. Geomagnetic excursions. In: Kono, M. (Ed.), *Treatise in Geophysics*, vol. 5. Elsevier, Amsterdam, pp. 373–416.
- Langereis, C.G., Hilgen, F.J., 1991. The Rossello composite: a Mediterranean and global reference section for the Early to early Late Pliocene. *Earth Planet Sci. Lett.* 104, 211–225.
- Laskar, J., Robutel, P., Joutel, F., Gastineau, M., Correia, A.C.M., Levrard, B., 2004. A long-term numerical solution for the insolation quantities of the Earth. *Astron. Astrophys.* 428, 261–285.
- Lentini, F., Carbone, S., 2014. *Geologia della Sicilia*. ISPRA. Mem. Descr.lla Carta Geol. Italia 95, 7–414.
- Lentini, F., Carbone, S., Catalano, S., Grasso, M., Monaco, C., 1991. Presentazione della carta geologica della Sicilia centro-orientale. *Mem. Soc. Geol. It.* 47, 145–156.
- Lepre, C.J., Kent, D.V., 2010. New magnetostratigraphy for the Olduvai subchron in the koobi fora formation, northwest Kenya, with implications for early Homo. *Earth Planet Sci. Lett.* 290 (3–4), 362–374.
- Lickorish, W.H., Grasso, M., Butler, R.W., Argnani, A., Maniscalco, R., 1999. Structural styles and regional tectonic setting of the “Gela Nappe” and frontal part of the Maghrebian thrust belt in Sicily. *Tectonics* 18 (4), 655–668.
- Lirer, F., Foresi, L.M., Iaccarino, S.M., Salvatorini, G., Turco, E., Cosentino, C., Sierro, F.J., Caruso, A., 2019. Mediterranean Neogene planktonic foraminifer biozonation and biochronology. *Earth Sci. Rev.* 196, 102869. <https://doi.org/10.1016/j.earscirev.2019.05.013>.
- Lisiecki, L.E., Raymo, M.E., 2005. A Pliocene-Pleistocene stack of 57 globally distributed benthic $\delta^{18}O$ records. *Paleoceanography* 20, PA1003. <https://doi.org/10.1029/2004PA001071>.
- Lourens, L.J., Hilgen, F.J., Gudjonsson, J., Zachariasse, W.J., 1992. Late Pliocene to Early Pleistocene astronomically-forced sea surface productivity and temperature variations in the Mediterranean. *Mar. Micropaleontol.* 19, 49–78.
- Lourens, L.J., Antonarakou, A., Hilgen, F.J., Van Hoof, A.A.M., Vergnaud-Grazzini, C., Zachariasse, W., 1996. Evaluation of the Plio-Pleistocene astronomical time-scale. *Paleoceanography* 11, 391–413. <https://doi.org/10.1029/96PA02691>.
- Lourens, L., Hilgen, F.J., Shackleton, N.J., Laskar, J., Wilson, D., 2004. The Neogene period. In: *A Geologic Time Scale 2004*. <https://doi.org/10.1017/CBO9780511536045.022>.
- Lyell, C., 1833. *Principles of Geology*, first ed., vol. III. John Murray, London, p. 393.
- Mayer-Eymar, K., 1858. Versuch einer neuen Klassifikation der Tertiär gebilde Europa's. *Verhandl. der Allgemeinen Schweiz. Ges. f. gesamt. Naturwissensch., Trogen*, pp. 165–199.
- Mayewski, P.A., Meeker, L.D., Twickler, M.S., Whitlow, S., Yang, Q., Lyons, W.B., Prentice, M., 1997. Major features and forcing of high-latitude northern hemisphere atmospheric circulation using a 110,000-year-long glaciochemical series. *J. Geophys. Res.*: Oceans 102 (C12), 26345–26366.
- Motta, S., 1957. Nota descrittiva geologica della tavoletta “Agrigento” (271-IV NE). *Boll. Serv. Geol. It.* 78, 519–567.
- Ogniben, L., 1969. Schema introduttivo alla geologia del Confine calabro-lucano. *Mem. Soc. Geol. It.* 8, 453–763.
- Pareto, M., 1865. Sur les subdivisions que l'on pourrait Établir dans les terrains Tertiaires de l'Apennin septentrional. *Bull. Soc. Géol. France* 22, 210–277.
- Pasini, G., Selli, R., Tampieri, R., Colalongo, M.L., D'Onofrio, S., Borsetti, A.M., Cati, F.M., 1975. The Vrica section. In: Selli, R. (Ed.), *The Neogene-Quaternary Boundary*, II Symposium (Bologna-Crotone), Excursion Guide-Book.
- Pasini, G., Colalongo, M.L., 1997. The Pleistocene boundary stratotype at Vrica, Italy. In: Van Couvering, J.A. (Ed.), *The Pleistocene Boundary and the Beginning of the Quaternary*. Cambridge University Press, Cambridge, pp. 15–45.
- Perch-Nielsen, K., 1985. Cenozoic calcareous nannofossils. In: Bolli, H.M., Saunders, J.B., Perch-Nielsen, K. (Eds.), *Plankton Stratigraphy*. Cambridge University Press, pp. 427–554.
- Pinter, P.R., Butler, R.W.H., Hartley, A.J., Maniscalco, R., Baldassini, N., Di Stefano, A., 2016. The Numidian of Sicily revisited: a thrust-influenced confined turbidite system. *Mar. Petrol. Geol.* 78, 291–311.
- Pinter, P.R., Butler, R.W.H., Hartley, A.J., Maniscalco, R., Baldassini, N., Di Stefano, A., 2018. Tracking sand-fairways through a deformed turbidite system: the numidian (Miocene) of central sicily, Italy. *Basin Res.* 30 (3), 480–501. <https://doi.org/10.1111/bre.12261>.
- Raffi, I., Backman, J., Fornaciari, E., Pälike, H., Rio, D., Lourens, L., Hilgen, F., 2006. A review of calcareous nannofossil astrobiochronology encompassing the past 25 million years. *Quat. Sci. Rev.* 25, 3113–3137. <https://doi.org/10.1016/j.quascirev.2006.07.007>.
- Raffi, I., Backman, J., Rio, D., Shackleton, N.J., 1993. Plio-pleistocene nannofossil biostratigraphy and calibration to oxygen isotope stratigraphies from deep sea drilling project site 607 and ocean drilling program site 677. *Paleoceanography* 8, 387–408. <https://doi.org/10.1029/93PA00755>.
- Raffi, S., Rio, D., Sprovieri, R., Valleri, G., Monegatti, P., Raffi, I., Barrier, P., 1989. New stratigraphic data on the Piacenzian stratotype. *Boll. Soc. Geol. It.* 108, 183–196.
- Raffi, I., Thunell, R., 1996. Comparison of the laminated units at Vrica and deep-sea sapropels from the eastern Mediterranean. In: Van Couvering, J. (Ed.), *The Pleistocene Boundary and the Beginning of the Quaternary*. Cambridge University Press, pp. 57–62. <https://doi.org/10.1017/cbo9780511585760.006>.
- Raffi, I., Wade, B.S., Pälike, H., Beu, A.G., Cooper, R., Crundwell, M.P., Krijgsman, W., Moore, T., Raine, I., Sardella, R., Vemyhorova, Y.V., 2020. Chapter 29 - the Neogene Period. In: Gradstein, F.M., Ogg, J.G., Schmitz, M.D., Ogg, G.M. (Eds.), *The Geological Time Scale 2020*. Elsevier, Amsterdam, Netherlands, pp. 1141–1215. <https://doi.org/10.1016/C2020-1-02369-3>, 2020.
- Rio, D., 1982. The fossil distribution of *Coccolithophore* Genus *Gephyrocapsa* Kamptner and related Plio-Pleistocene chronostratigraphic problems. In: Prell, W.L., Gardner, J.V., et al. (Eds.), *Init. Repts. DSDP*, 68. U.S. Govt. Printing Office), Washington, pp. 903–910. <https://doi.org/10.2973/dsdp.proc.68.109.1982>.
- Rio, D., Channell, J.E.T., Bertoldi, R., Poli, M.S., Vergerio, P.P., Raffi, I., Sprovieri, R., Thunell, R.C., 1997a. Pliocene sapropels in the northern Adriatic area: chronology and paleoenvironmental significance. *Palaeogeogr. Palaeoclimatol. Palaeoecol.* 135 (1–4), 1–225. [https://doi.org/10.1016/S0031-0182\(97\)00027-8](https://doi.org/10.1016/S0031-0182(97)00027-8).
- Rio, D., Raffi, I., Villa, G., 1990. Pliocene-Pleistocene calcareous nannofossil distribution patterns in the western Mediterranean. In: Kastens, K.A., Mascle, J., et al. (Eds.), *Proc. ODP, Sci. Results*, vol. 107. Ocean Drilling Program), College Station, TX, pp. 513–533. <https://doi.org/10.2973/odp.proc.sr.107.164.1990>.
- Rio, D., Sprovieri, R., Raffi, I., 1984. Calcareous plankton stratigraphy and biochronology of the pliocene-lower Pleistocene succession of the Capo Rossello area, sicily. *Mar. Micropaleontol.* 9, 135–180. [https://doi.org/10.1016/0377-8398\(84\)90008-2](https://doi.org/10.1016/0377-8398(84)90008-2).
- Rio, D., Sprovieri, R., Di Stefano, E., 1994. The Gelasian Stage: a proposal of a new chronostratigraphic unit of the Pliocene Series. *Riv. Ital. Paleontol. Stratigr.* 100, 103–124.
- Rio, D., Sprovieri, R., Raffi, I., Valleri, G., 1988. Biostratigrafia e paleoecologia della sezione stratotipica del Piacenziano. *Boll. Soc. Geol. Ital.* 27, 213–238.
- Rio, D., Sprovieri, R., Thunell, R.C., 1991. Pliocene-lower Pleistocene chronostratigraphy: a re-evaluation of Mediterranean type sections. *Geol. Soc. Am. Bull.* 103, 1049–1058. [https://doi.org/10.1130/0016-7606\(1991\)103<1049:PLPCAR>2.3.CO;2](https://doi.org/10.1130/0016-7606(1991)103<1049:PLPCAR>2.3.CO;2).
- Rio, D., Raffi, I., Backman, J., 1997b. Calcareous nannofossil biochronology and the Pliocene/Pleistocene boundary: the Neogene/Quaternary boundary. In: Van Couvering, J.A. (Ed.), *The Pleistocene Boundary and the Beginning of the Quaternary: Final Report of the International Geological Correlation Program-Project 41, Neogene-Quaternary Boundary*. Cambridge. Cambridge Univ. Press, pp. 63–78.
- Rio, D., Sprovieri, R., Castradori, D., Di Stefano, E., 1998. The Gelasian Stage (Upper Pliocene): a new unit of the global standard chronostratigraphic scale. *Episodes* 21 (2), 82–87. <https://doi.org/10.18814/epiiugs/1998/v21i2/002>.
- Roberts, A.P., Chang, L., Rowan, C.J., Hornig, C.S., Florindo, F., 2011. Magnetic properties of sedimentary greigite (Fe₃S₄): an update. *Rev. Geophys.* 49, RG1002. [https://doi.org/10.1016/0012-821X\(95\)00131-U](https://doi.org/10.1016/0012-821X(95)00131-U).
- Roberts, A.P., Florindo, F., Larrasoana, J.C., O'Regan, M.A., Zhao, X., 2010. Complex polarity pattern at the former Plio-Pleistocene global stratotype section at Vrica (Italy): remagnetization by magnetic iron sulphides. *Earth Planet Sci. Lett.* 292 (1–2), 98–111.
- Roda, C., 1964. Distribuzione e facies dei sedimenti Neogenici nel Bacino Rotoneo. *Geol. Rom.* 3, 319–366.
- Rohling, E., Foster, G., Grant, K., Marino, G., Roberts, A.P., Tamisiea, M.E., Williams, F., 2014. Sea-level and deep-sea-temperature variability over the past 5.3 million years. *Nature* 508, 477–482. <https://doi.org/10.1038/nature13230>.
- Rohling, E.J., Marino, G., Grant, K., 2015. Mediterranean climate and oceanography, and the periodic development of anoxic events (sapropels). *Earth Sci. Rev.* 143, 62–97.
- Ruggieri, G., Greco, A., 1966. Distribuzione dei macrofossili nel Calabro inferiore di Agrigento. *Atti Acc. Gioenia Sc. Nat.* 18, 319–327.
- Sagnotti, L., Roberts, A.P., Weaver, R., Verosub, K.L., Florindo, F., Pike, C.R., Clayton, T., Wilson, G.S., 2005. Apparent magnetic polarity reversals due to remagnetization resulting from late diagenetic growth of greigite from siderite. *Geophys. J. Int.* 160, 89–100. <https://doi.org/10.1111/j.1365-246X.2005.02485.x>.
- Salvador, A. (Ed.), 1994. *International Stratigraphic Guide: a Guide to Stratigraphic*

- Classification, Terminology, and Procedure (No. 30). Geological Society of America, p. 214.
- Schiebel, R., Hemleben, C., 2017. *Planktic Foraminifers in the Modern Ocean*. Springer-Verlag GmbH Berlin Heidelberg. <https://doi.org/10.1007/978-3-662-50297-6>.
- Shackleton, N.J., Backman, J., Zimmerman, H.T., Kent, D.V., Hall, M.A., Roberts, D.G., et al., 1984. Oxygen isotope calibration of the onset of ice-rafting and history of glaciation in the North Atlantic region. *Nature* 307 (5952), 620–623.
- Selli, R., Accorsi, C.A., Bandini Mazzanti, M., Bertolani Marchetti, D., Bonadonna, F.P., Borsetti, A.M., Cati, F., Colalongo, M.L., d'Onofrio, S., Landini, W., Menesini, E., Mezzetti, R., Pasini, G., Savelli, G., Tampieri, R., 1977. The Vrica section (Calabria). A potential Neogene-Quaternary boundary stratotype. *G. Geol. (Bologna)* 41, 181–204.
- Singer, B.S., Jicha, B.R., Condon, D., Macho, A., Hoffman, K.A., Brown, M., Feinberg, J., Kidane, T., 2014. Precise ages of the Réunion event and Huckleberry Ridge excursion: episodic clustering of geomagnetic instabilities and the dynamics of flow within the outer core. *Earth Planet Sci. Lett.* 405, 25–38.
- Spaak, P., 1983. Accuracy in correlation and ecological aspects of the planktonic foraminiferal zonation of the Mediterranean Pliocene: utrecht Micropaleontol. Bull. (Arch. Am. Art) 28, 1–159.
- Sprovieri, R., 1992. Mediterranean Pliocene biochronology: a high-resolution record based on quantitative planktonic foraminifera distribution. *Riv. Ital. Paleontol. Stratigr.* 98, 61–100.
- Sprovieri, R., 1993. Pliocene-Early Pleistocene astronomically forced planktonic foraminifera abundance fluctuations and chronology of Mediterranean calcareous plankton bio-events. *Riv. Ital. Paleontol. Stratigr.* 99, 371–414.
- Sprovieri, R., Thunell, R., Howell, M., 1986. Paleontological and geochemical analysis of three laminated sedimentary units of late Pliocene-early Pleistocene age from the Monte san Nicola section in sicily. *Riv. Ital. Paleontol. Stratigr.* 92, 401–434.
- Sprovieri, R., Di Stefano, E., Howell, M., Sakamoto, T., Di Stefano, A., Marino, M., 1998. Integrated calcareous plankton biostratigraphy and cyclostratigraphy at Site 964. In: Robertson, A.H.F., Emeis, K.-C., Richter, C., Camerlenghi, A. (Eds.), *Proc. ODP, Sci. Results*, vol. 160. Ocean Drilling Program, College Station, TX, pp. 155–165. <https://doi.org/10.2973/odp.proc.sr.160.010.1998>.
- Sprovieri, R., Di Stefano, E., Incarbona, A., Oppo, D.W., 2006. Suborbital climate variability during Marine Isotopic Stage 5 in the central Mediterranean basin: evidence from calcareous plankton record. *Quat. Sci. Rev.* 25, 2332–2342.
- Tauxe, L., Opdyke, N.D., Pasini, G., Elmi, C., 1983. Age of the plio-pleistocene boundary in the Vrica section, southern Italy. *Nature* 304, 125–129.
- Thierstein, H.R., Geitzenauer, K.R., Molino, B., Shackleton, N.J., 1977. Global synchronicity of late Quaternary coccolith datum levels: validation by oxygen isotopes. *Geology* 5, 400–404.
- Toucanne, S., Zaragosi, S., Eynaud, F., Bourillet, J.F., Lericolais, G., Gibbard, P.L., 2011. Comments to westaway and Bridgland-Causes, consequences and chronology of large-magnitude palaeoflows in middle and late Pleistocene river systems of northwest europe. *Earth Surf. Process. Landforms* 36 (10), 1410–1413.
- Van Couvering, J.A., Castradori, D., Cita, M.B., Hilgen, F.J., Rio, D., 2000. The base of the zanclean stage and of the Pliocene series. *Episodes* 23 (3), 179–187.
- Verhallen, P.J.J.M., 1987. Early development of *Bulimina marginata* in relation to paleoenvironmental changes in the Mediterranean. *Proc. Ned. Akad. Wet.* 90, 161–180.
- Vitale, F., 1996. I Bacini plio-pleistocenici della Sicilia: Un laboratorio naturale per lo studio delle interazioni tra tettonica e glacioeustatismo. *Riun. Gr. Sediment. CNR-Guida alle escursioni*. In: Colella, A. (Ed.), pp. 61–116.
- Walsh, S.L., Gradstein, F.M., Ogg, J.G., 2004. History, philosophy, and application of the global stratotype section and point (GSSP). *Lethaia* 37, 201–218.
- Walsh, S.L., 2008. The Neogene: origin, adoption, evolution, and controversy. *Earth Sci. Rev.* 89, 42–72.
- Young, J.R., Bown, P.R., Lees, J.A., 2017. *Nannotax3 Website*. International Nannoplankton Association. <https://www.mikrotax.org/Nannotax3>. (Accessed 21 April 2017).
- Zachariasse, W.J., Gudjonsson, L., Hilgen, F.J., Langereis, C., 1990. Late Gauss to early Matuyama invasions of *Neoglobobulimina atlantica* in the mediterranean and associated record of climatic change. *Paleoceanography* 5, 239–252.
- Zijderveld, J.D.A., 1967. AC demagnetization of rocks: analysis of results. In: Runcorn, S.K., Creer, K.M., Collinson, D.W. (Eds.), *Methods in Palaeomagnetism*. Elsevier, Amsterdam, pp. 254–286.
- Zijderveld, J.D.A., Hilgen, F.J., Langereis, C.G., Verhallen, P.J.J.M., Zachariasse, W.J., 1991. Integrated magnetostratigraphy and biostratigraphy of the upper pliocene-lower Pleistocene from the Monte Singa and Crotona areas in Calabria (Italy). *Earth Planet Sci. Lett.* 107, 697–714.